THESIS FOR THE DEGREE OF DOCTOR OF PHILOSOPHY

On Methods for Probing Structure and Function of Membrane Proteins

ERIK T. JANSSON

Department of Chemical and Biological Engineering
CHALMERS UNIVERSITY OF TECHNOLOGY
Göteborg, Sweden 2012

On Methods for Probing Structure and Function of Membrane Proteins
ERIK T. JANSSON

ISBN: 978-91-7385-784-0

Doktorsavhandlingar vid Chalmers tekniska högskola
Ny serie nr 3465
ISSN: 0346-718X

Department of Chemical and Biological Engineering
Chalmers University of Technology
SE-412 96 Göteborg
Sweden
Telephone: +46-(0)31 772 1000

Front cover image: “The gatekeepers”
Back cover photo by Alar Ainla

Printed by Chalmers reproservice
Göteborg, Sweden 2012

On Methods for Probing Structure and Function of Membrane Proteins

ERIK T. JANSSON
Department of Chemical and Biological Engineering
Chalmers University of Technology

Abstract

The determination of structure–function relationships in membrane proteins plays a key role for the understanding of molecular mechanisms in biological systems, and may provide information on how these systems can be modulated by pharmaceuticals. The aim of the work described herein was to develop methods for studying structure and function of membrane proteins, ideally in combination. The ion channel TRPV1 expressed in Chinese hamster ovary (CHO) cells was used as a model system for evaluation of the methods developed, and further investigations of structure–function relationships in TRPV1 were conducted with these methods. First, a new method for studying ion channel activation was developed based on a microfluidic pipette fabricated in poly(dimethylsiloxane). This device is able to generate a confined volume zone in front of the pipette, and can provide chemical dilution series for the measurement of concentration-response curves in pharmacological studies of cells. The pipette supports delivery of multiple solutions, and rapid switching (<100 ms) between solutions is readily achieved. Second, the pipette was applied in a study were depletion of cholesterol content of cell membranes was found to modulate TRPV1 function under hypocalcemic conditions. The effect of cholesterol-depletion on TRPV1 function was measured with patch-clamp and a fluorescence assay. The treatment was found to inhibit the dynamic permeability of TRPV1 for large cations. Third, a microfluidic flow cell, in which proteoliposomes can be immobilized, was characterized and further developed for use with limited proteolysis. A sequential digestion protocol for proteomic analysis with mass spectrometry of membrane proteins was innovated, where a stationary phase of proteoliposomes derived from CHO-cells was repeatedly exposed to trypsin inside the flow cell channel, and the peptides resulting from each digestion step were used for protein identification. This protocol was found to increase the amount of identified membrane proteins compared to a single-digest protocol, when performing bottom-up proteomic analysis. Finally, a method for the determination of structure–function interconnections in ion channels, combining limited proteolysis with mass spectrometry and patch-clamp recording of ion channel activity, was able to identify distal parts of the TRPV1 protein which are not engaged in activation of the channel with capsaicin.

Keywords: Membrane proteins, TRPV1, patch-clamp, fluorescence, cholesterol, microfluidic superfusion, proteoliposomes, proteomics, limited proteolysis, mass spectrometry.

List of Publications

This thesis is based on the work presented in the research papers below, which are referred to as Paper I–IV in the text.

I Ainla, A., Jansson, E. T., Stepanyants, N., Orwar, O., and Jesorka, A. (2010) A microfluidic pipette for single-cell pharmacology. *Anal. Chem. 82*, 4529–4536.

II Jansson, E. T., Trkulja, C. L., Ahemaiti, A., Millingen, M., Jeffries, G. D. M., Jardemark, K., and Orwar, O. Effect of cholesterol depletion on the pore dilation of TRPV1. *Manuscript*.

III Jansson, E. T., Trkulja, C. L., Olofsson, J., Millingen, M., Wikström, J., Jesorka, A., Karlsson, A., Karlsson, R., Davidson, M., and Orwar, O. (2012) Microfluidic flow cell for sequential digestion of immobilized proteoliposomes. *Anal. Chem. 84*, 5582–5588.

IV Trkulja, C. L., Jansson, E. T., Jardemark, K., and Orwar, O. Probing structure and function of ion channels using limited proteolysis. *Manuscript*.

Contribution Report

My contribution to the papers appended in this thesis is as follows:

I I contributed partially with experiments, and discussion of the results.

II I contributed partially with experiments. I planned the experiments and wrote the paper.

III I contributed partially, with modelling, planning, and experiments. I wrote the paper.

IV I contributed partially, with planning, experiments, and discussion of the results.

Contents

1 Introduction

> Either write something worth reading or do something worth writing.
>
> *(Benjamin Franklin)*

Understanding how the structure of membrane proteins relates to their function, is a key pathway to elucidate the mechanisms by how these proteins perform their tasks in a biological cell. Such knowledge, along with insights into the role of protein dysfunction in diseases, is important in the field of drug discovery [1–4].

The prediction of the three-dimensional conformation of membrane proteins is possible, as peptide sequences for many proteins are readily available today. However, calculations which predict protein folding are still difficult to achieve for proteins with more than 150 amino acid residues [5, 6]. Further, experimental studies of membrane protein structure, investigating conformation dynamics, its interaction with ligands, and how this interconnection in turn rule its function, have been performed in some instances with X-ray crystallography and NMR studies, e.g. for ion channels and G-protein coupled receptors [1, 3, 7–10]; work for which Roderick MacKinnon and Brian Kobilka received the Nobel prize in chemistry in 2003 and 2012, respectively. However, the hydrophobic nature of membrane proteins complicates this task, as these techniques in general require the use of detergents and organic solvents, and membrane proteins are also very difficult to crystallize. Further, these techniques require in general large amounts of sample; a challenge for work with membrane proteins which often naturally exist only in low abundance in a cell [8, 10]. Membrane proteins represent up to 70% of existing drug targets, but determination of their structure has to date yet only been modest [4], e.g. only a small fraction of membrane proteins expressed in mammalian hosts have had their structure determined with X-ray crystallography [11]. Another technique which may contribute to the field of structural biology, is mass spectrometry which has been proven to be a suitable method for probing structure and dynamics of membrane proteins. Mass spectrometry can handle heterogenous and complex protein samples, hence not requiring purification of the protein of interest, and require only small amounts of sample for analysis, a bottleneck in X-ray crystallography and NMR studies [12–18]. This methodology relies on the fragmentation of proteins prior to analysis, and detection of the resulting peptides yield structural information. Limited proteolysis of proteins, an approach where digestion is only partially performed, has e.g. been able to determine relations between structure and activity of enzymes. Partnered with mass spectrometry, limited proteolysis can provide details of the topology and peptide chain flexibility of membrane proteins [12, 19].

Functional studies of ion channels, a subset of membrane proteins considered as very potent drug targets, may provide more understanding of how various environmental and chem-

ical stimuli, e.g. drugs, modulate and determine their actions. Methods for relating structure with function may in turn extend our knowledge of the regulation of biological responses and diseases [20, 21]. Patch-clamp is an electrophysiological technique regarded as the golden standard for probing the function of ion channels [22–27]. The recording of single-channel currents with patch-clamp allows kinetic models to be imposed on the ion channel, and pharmacological studies can be performed with this technique [28–33].

The work described herein aimed to contribute to the development of techniques for probing both structure and function of membrane proteins, and to investigate the interplay of these features, which are closely related. The studies were conducted with fluorescence, patch-clamp, and mass spectrometry measurements, all in combination with the innovation of microfluidic devices. This setup provided the ability to correlate structural changes with activity dynamics in the nociceptive ion channel TRPV1.

2 Membrane Proteins

> Le nom protéine que je vous propose pour l'oxyde organique de la fibrine et de l'albumine, je voulais le dériver de πρωτειος, parce qu'il paraît être la substance primitive ou principale de la nutrition animale que les plantes préparent pour les herbivores, et que ceux-ci fournissent ensuite aux carnassiers.
>
> *(Jöns Jacob Berzelius)*

Proteins are responsible for carrying out a vast amount of operations in a biological cell, e.g. by mediating transportation of nutrients and salts, metabolism, and extracellular signaling. The cell is an enclosed compartment, where DNA, RNA, proteins, nutrients and salts are enveloped by a lipid bilayer, i.e. the plasma membrane. Further compartmentalization is achieved by organelles, where envelopes of lipid bilayer within the cell provide a separation of biochemical reactions and cellular storages from each other. However, transportation of ions and other molecules necessary for sustaining cell signaling and metabolism, is not possible to perform by diffusion across the cell membrane. These processes are facilitated in the cell by membrane proteins, forming physical transport gates across the membrane. The work of this thesis regards studies of membrane proteins, where development of methods for membrane protein analysis, and investigations on how chemical modification may alter ion channel functionality, have been concerned.

2.1 Structure and Function

Proteins are molecules constructed by the linking of amino acid chains, which sequence is provided by the genetic information stored in the DNA of a cell, as the DNA is encoded into the primary structure of a protein. The peptide sequence will in turn determine how the protein will fold, hence, it also determines the function of the protein. The relation between translation of a protein from RNA, and the transcription of RNA from DNA constitutes the central dogma of molecular biology [34]. Further, proteins are divided into three main groups; globular proteins, fibrous proteins, and membrane proteins. Almost all globular proteins are aqueous, i.e. they reside freely in solution, and are usually enzymes. Fibrous proteins, e.g. collagen and elastin, provide structure to the extracellular matrix of a cell. Membrane proteins are partly or wholly associated in various ways with a membrane of the cell, and often act as receptors.

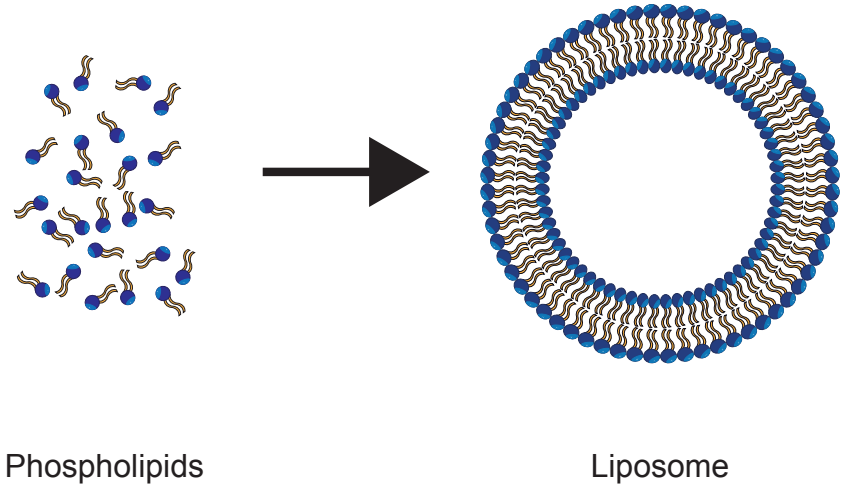

Figure 2.1: Schematic illustration of a group of phospholipids in aqueous solution, which spontaneously can arrange into a liposome to minimize the Gibbs free energy of the system.

Membrane proteins can be covalently associated with the lipid bilayer, e.g. through lipidation of an amino acid. Transmembrane proteins can extend through the lipid bilayer as a single or a multi-pass α-helix, or as a β-barrel [35, 36]. These peptide chains can together with either similar or different subunits form a three-dimensional conformation, which together provide the complete structure and function of a membrane protein.

2.2 Lipid Bilayers

Phospholipids are amphiphilic molecules with a hydrophobic tail and a hydrophilic headgroup. When immersed in aqueous solution, phospholipids can spontaneously form an enclosed compartment by arranging themselves into a lipid bilayer, e.g. a liposome, to minimize the Gibbs free energy of the system (Figure 2.1). The function of proteins can depend on the fluidity of the membrane they reside within, which is modulated by lipid composition and the presence of sterols, e.g. cholesterol [37–40]. Some lipids with saturated hydrocarbon chains can adhere so strongly that microdomains are formed, i.e. lipid rafts, which also are rich of cholesterol. Lipid rafts are considered to promote the organization of a subset of membrane proteins and to regulate protein–protein interactions, as membrane proteins tend to accumulate in these fatty microdomains [35, 36, 38, 41–44]. A method for rapid decrease or delivery of sterols to the lipid bilayer of a cell, is the employment of cyclodextrins, used for studying effects of membrane fluidity or sterol interaction with membrane proteins [37–40, 43, 45, 46]. The extent of sterol modulation can be quantitated with fluorescent assays or with gas-chromatographic methods [47–51].

Table 2.1: Ion concentrations and thermodynamic equilibrium potentials for a mammalian skeletal muscle cell. Adapted from Hille [52].

Ion	Extracellular concentration (mM)	Intracellular concentration (mM)	Equilibrium potential (mV)
Na^+	145	12	67
K^+	4	155	−98
Ca^{2+}	1.5	10^{-7}	129
Cl^-	123	4.2	−90

2.3 Ion Channels

The lipid bilayer of a cell is impermeable to ions, as the charge carried by ions makes it difficult to diffuse across the hydrophobic plasma membrane. Transportation is mediated through pore forming proteins, i.e. ion channels, which are usually selective for one or many types of ions.

The mechanism for opening an ion channel, i.e. gating, can be triggered by changes in membrane potential, the binding of a ligand, mechanical stimuli, through second messenger molecules, by temperature, or by combinations of these events. Ion channels enable cells to communicate with each other, as a stimuli causing the opening of a specific ion channel may initialize a signal cascade, e.g. propagation of an action potential along a nerve.

2.3.1 Membrane Potential

The hydrophobic nature of the plasma membrane of a cell, renders it impermeable to charged molecules. Hence, the physical separation of charged species across the membrane, is equivalent to that found in an electric capacitor. The resulting voltage, known as the thermodynamic equilibrium potential E_S, is described by the Nernst equation,

$$E_S = \frac{RT}{z_S F} \ln \frac{S_{out}}{S_{in}}, \tag{2.1}$$

where R is the gas constant, T is the temperature, F is Faraday's constant, z_S is the ion-valency, and S_{out} and S_{in} are the extra- and intracellular concentrations, respectively, of an ion for which the membrane is specifically permeable to. Typically, for a non-excited cell at rest, extra- and intracellular concentrations for cells are not at equilibrium, as active pumps transport ions out- and inwards to maintain an electrochemical gradient. The thermodynamic equilibrium potentials for different ions in a mammalian cell are given in Table 2.1.

The resting membrane potential under the assumption that the membrane is only permeable to Na^+, K^+ and Cl^-, calculated as the reversal potential E_{rev} at which no net current flows, is given by the Goldman–Hodgkin–Katz voltage equation,

$$E_{rev} = \frac{RT}{F} \ln \left(\frac{\sum_i^N P_{M_i^+} [M_i^+]_{out} + \sum_j^M P_{A_j^-} [A_j^-]_{in}}{\sum_i^N P_{M_i^+} [M_i^+]_{in} + \sum_j^M P_{A_j^-} [A_j^-]_{out}} \right), \tag{2.2}$$

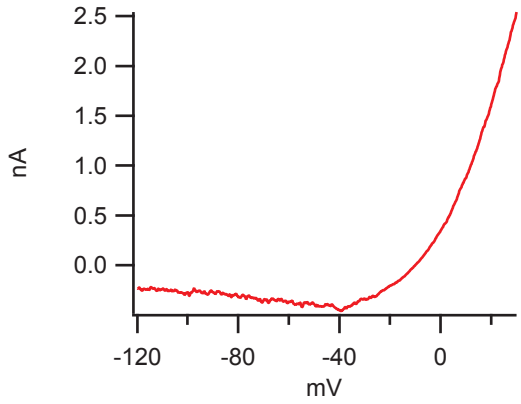

Figure 2.2: Current-voltage relationship for TRPV1 with external and internal sodium buffers during activation with 1 µM capsaicin, measured with a ramp protocol from −120 mV to 30 mV over 150 ms. The ion channel rectifies the current readily in the range of −120 to −40 mV.

where P denotes the ion-specific permeability, and M^+ and A^- are cations and anions, respectively. Given the values in Table 2.1, and knowing that mainly K^+-channels are open at rest, the resting potential is calculated to be ~ -90 mV, close to the equilibrium potential of K^+.

2.3.2 Current-Voltage Relations in Channels

The membrane of a cell behaves like a capacitor, and an ion channel behaves as a conductor. However, due to the concentration gradient of ions across the membrane, current will drop to zero at the reversal potential, not at 0 mV. The membrane conductance can also be directly dependent on voltage, i.e. it displays rectification, where the ion channel will be open and permeate ions at some membrane potentials, and remain closed at others (Figure 2.2).

2.3.3 Permeability

Sodium and potassium ions are both monatomic and monovalent cations, their effective ionic radii differ by only 0.4 Å, and yet, their ability to permeate through an ion channel can be very different, e.g. potassium is 10 000 times more permeant than sodium in certain potassium channels due to selectivity filters [3, 53–55].

Ion channels are usually selective for the types of ions they will permeate, which has resulted in classifications of ion channels according to the mainly conducted ion e.g. the families of Na^+-, K^+-, and Cl^--channels.

Relative ion selectivity can be measured by experiments conducted in parallel, e.g. with different types of ions on the outside of the cell. The reversal potential for each of these two

conditions can then be described as

$$E_{rev}^{A} = \frac{RT}{F} \ln \frac{P_A[A]_{out}}{P_C[C]_{in}} \tag{2.3}$$

$$E_{rev}^{B} = \frac{RT}{F} \ln \frac{P_A[B]_{out}}{P_C[C]_{in}}. \tag{2.4}$$

If Equation 2.3 is side subtracted with Equation 2.4, and the exponential function is applied to both sides, the expression gives the relative permeability of A to B as

$$\frac{P_A}{P_B} = \frac{[A]_{out}}{[B]_{out}} \exp \frac{\Delta E_{rev} F}{RT}. \tag{2.5}$$

2.3.4 Nerve Signaling

Cells which can utilize changes in membrane potential for communication are called excitable cells, e.g. nerve- and muscle cells can in response to their changes in membrane potential induce release of neurotransmitters or muscle contraction. An increase of membrane potential is referred to as depolarization, whereas a decrease is referred to as hyperpolarization. If, e.g. a nerve cell is depolarized above a certain threshold level, an action potential is triggered, i.e. a change in membrane potential is caused at a certain locus of a nerve cell (the axon hillock), which will propagate along the entire cell, to the nerve terminal. In detail, this occur by activation of Na^+-channels upon depolarization, which further depolarizes the cell membrane, since the equilibrium potential of Na^+ is $\sim$67 mV. The local depolarization will spread electrotonically in the adjacent membrane area, which causes activation of Na^+-channels further down in the cell. Upon depolarization, K^+-channels are also activated, which however are $\sim$1 ms slower than Na^+-channels, and cause hyperpolarization of the cell membrane since the equilibrium potential of K^+ is ~ -98 mV. Once the K^+-channels close, the membrane potential returns to its resting value as the sodium-potassium pump restore the chemical gradient at the cost of ATP. Once the action potential has reached the end of a nerve cell, the electric signal must be chemically converted to cross the synapse, a gap between two adjacent nerve cells, and reach the dendrites of the adjacent nerve cell. This conversion is performed by the release of a chemical transmitter in the presynaptic cell, which diffuse across the synaptic cleft and bind to receptors on the postsynaptic side, which activate and cause an action potential to be triggered in the next nerve cell [56]. An equivalent circuit showing current flow in the cell membrane is given in Figure 2.3.

2.3.5 Ion Channel Kinetics

The simplest model of ion channel kinetics describe the transition between a closed and opened state, e.g. when an agonist bind to an ion channel, it causes a conformational change of the ion channel which opens the channel, and holds it open for most of the time.

$$C \rightleftharpoons O. \tag{2.6}$$

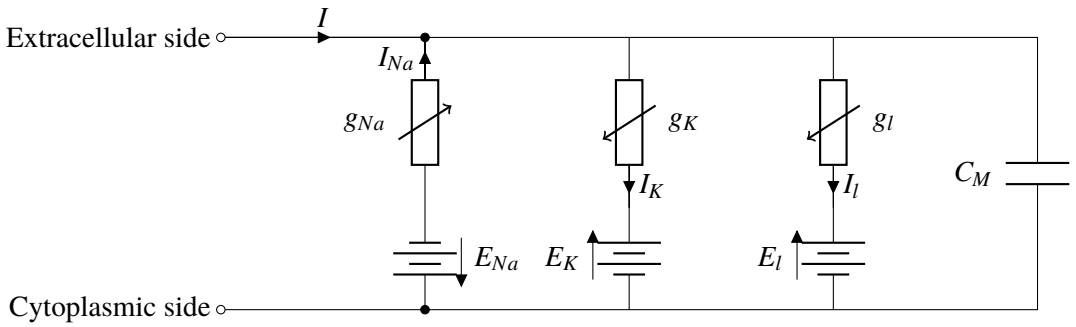

Figure 2.3: Equivalent circuit of a cell, the membrane capacitance C_M is determined by the properties of the lipid bilayer, the conductances g_{Na}, g_K, g_l is determined by the states (opened or closed) of the ion channels permeable for sodium, potassium, and other ions, respectively, and the voltages E_{Na}, E_K, E_l by the concentrations of the respective ion species of each side of the lipid bilayer. Adapted from Hodgkin and Huxley [57].

A reaction scheme for binding of a ligand to a receptor, separated from the opening event was first described by del Castillo and Katz [58],

$$R + L \rightleftharpoons RL \rightleftharpoons RL', \tag{2.7}$$

where R is the receptor, and L is the ligand, RL is the ligand-bound receptor, and RL' is the activated ligand-bound receptor. This model mechanism can also used for inhibitory ligands, which are antagonists and close the ion channel. Hence, both binding and dissociation rates of ligands, and opening and closing rates of the ion channel, determine the activation of an ion channel. Further, there also exist partial agonists, which will bind the receptor and activate it, yet not unto full extent [32, 58].

2.3.6 Transient Receptor Potential Vanilloid 1

The mechanisms underlying the pain-evoking capacity of capsaicin, the pungent compound found in peppers of the *Capsicum* family (Figure 2.4), in mammalian cells and its interconnection with heat in the nervous system of the human body [59–63], was revealed by the cloning of the transient receptor potential vanilloid 1 (TRPV1) ion channel in 1997 by Caterina et al. [64]. TRPV1 is a key mediator of nociception and neurogenic inflammation [64–68], and is expressed in dorsal root ganglia and trigeminal ganglia, which are sensory neurons mediating signals from skin, muscles, and joints of the limbs and trunk to the spinal cord cluster in the dorsal root ganglia, immediately adjacent to the spinal cord [56, 69–71]. TRPV1 is a polymodal non-selective cation channel, i.e. it is voltage-gated, activated by a broad range of chemical stimuli which include protons, capsaicin, arachnoid toxin, and also environmental effects such as painfully hot temperatures (>42°C). TRPV1 is permeable not only for monovalent cations, but also for Ca^{2+} and other relatively large cations [64, 65, 71–80]. Hence, oral intake or topological application of capsaicin cause a burning sensation, as this agonist

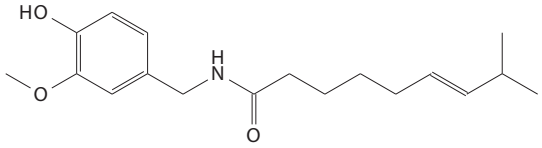

Figure 2.4: The molecular structure of capsaicin, the pungent compound found in peppers from the *Capsicum* family.

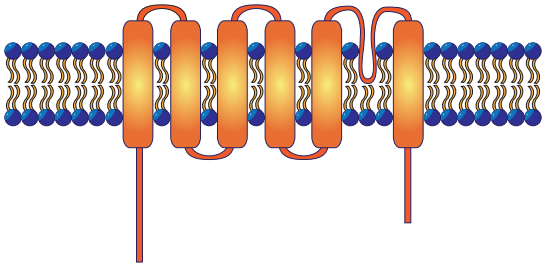

Figure 2.5: TRPV1 consists of six transmembrane regions, and has a transmembrane loop between TM5–6.

targets a receptor also activated by heat. It is notable that while avian TRPV1 is readily activated by acidic conditions and high temperature, it is insensitive to capsaicin in contrast to its mammalian orthologs [60, 81]. By these means, it seems that peppers chemically favour birds as seed dispersal vectors over other animals [82, 83].

The TRPV1 subunit consists of the six transmembrane domains with the binding site of capsaicin located on the cytosolic side [81, 84], the proton binding site has been located in the pore region [77], temperature regulation is determined by its distal ends but also by the pore turret [85, 86] (Figure 2.5). The structure of TRPV1 resemble the voltage-gated K^+-channel Kv1.2, which is constituted by four subunits, and has been probed by electron cryomicroscopy [87]. However, whereas a crystal structure has been determined for Kv1.2, a high-resolution structure exist only for parts of TRPV1 [7, 88].

TRPV1 is desensitized during activation in presence of intracellular calcium and calmodulin, but also via kinases [88–97]. Further examples of TRPV1 modulating molecules are ATP (which has been found to potentiate TRPV1 current, and to recover it from a desensitized state) [93, 98], protons (which potentiate TRPV1 and alter current kinetics) [99, 100], and glycosylation (which alter TRPV1 permeability) [101].

A noticeable feature of TRPV1 is its dynamic permeability for large cations, which changes over time during sustained activation of the ion channel with ligand. Such behaviour is however not unique, but still, there are only a few other ion channels which share this function with TRPV1, e.g. the P2X purinoceptor channels, and the TRPA1 ion channel [102–106]. However, in TRPV1 the heat-activation pathway does not induce such permeability changes, which confirms the complex behaviour of this polymodal receptor.

The expression of TRPV1 in nociceptors and the electrophysiological properties of the

channel, provides capability of the nervous system to mediate nociception and neurogenic inflammation. TRPV1 significantly contribute to the integration of the actions of various inflammatory modulators, which makes this ion channel a central regulator of nociceptor excitability. Consequently, the key role of TRPV1 in the onset and maintenance of neurogenic inflammation, has identified it as a potential drug target for alleviating inflammatory pain [68, 107–111].

3 Electrophysiological Techniques

> Admovi propterea & ipse scalpelli cuspidem uni vel alteri crurali nervo, quo tempore unus aliqui ex iis, qui aderant, scintillam eliceret. Phænomenon eadem omnio ratione contigit; vehementes nimirum contractiones in singulos artuum musculos, perinde ac si tetano præparatum animal esset correptum, eodem ipso temporis momento inducebantur, quo educebantur scintillæ.
>
> *(Luigi Aloisio Galvani)*

The study of electrical properties of biological cells and tissues, using electrophysiological techniques, provides information e.g. on how receptors and signaling work within the nervous system. The intracellular recording technique, developed by Hodgkin and Huxley in the 1930s, made recordings of the membrane potential possible, which enabled them to elucidate the mechanisms underlying action potentials in neurons [57, 112–115], work for which they received the Nobel prize in physiology and medicine in 1963.

3.1 Patch-Clamp Recording Configurations

Intracellular recording techniques require the insertion of electrodes into a cell, hence limiting the size of cells possible to study, and single-channel events are not possible to record. A decade after the award of Hodgkin's and Huxley's work, Sakmann and Neher with co-workers [22–24] presented a technique whereby single-channel currents could be measured, a discovery for which they received the Nobel prize in physiology and medicine in 1991.

The setup for patch-clamp includes a glass pipette usually made from borosilicate, which is filled with a salt solution, most often mimicking physiological conditions, and with an inserted silver wire (often coated with AgCl) which is connected to a patch-clamp amplifier via a headstage. For experiments, a reference electrode is immersed into a cell dish or similar filled with a physiological salt solution, followed by the glass pipette with a small applied pressure in it, to avoid debris clogging the tip. An inverted microscope placed on a vibration damping table is utilized for visual orientation when approaching a cell with the glass pipette. The ap-

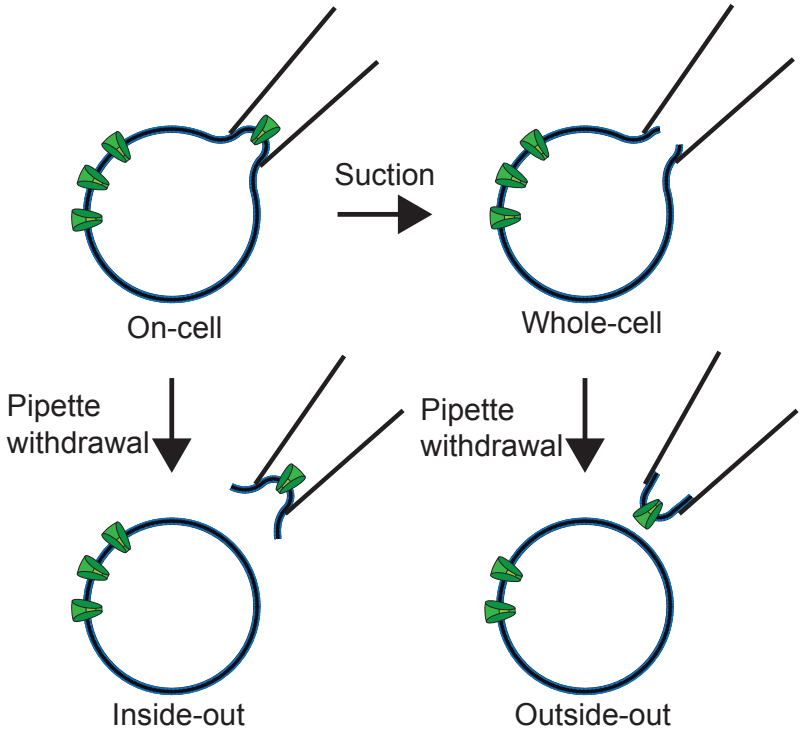

Figure 3.1: Patch-clamp pipette configurations. The formation of a gigaseal between the pipette and a cell achieves the on-cell mode, from which the other recording modes can be obtained. Adapted from Hamill et al. [24] and Hille [52].

plied pressure is released and the pipette is then brought into contact with the cell membrane (optionally suction can be applied, see Figure 3.1), whereupon formation of a gigaohm-seal may occur [116–118]. This seal is both electrically and mechanically stable, and is referred to as a cell-attached or on-cell mode. The establishment of a gigaohm-seal is crucial for patch-clamp experiments, as a cell–pipette seal with a resistance of less than ~ 1 GΩ would yield leak currents and increased noise in the measurements. From the on-cell configuration, one may continue to other recording modes, e.g. an inside-out patch configuration can be achieved by pulling the pipette away from the cell. Furthermore, by applying suction immediately after achieving the on-cell mode, a whole-cell configuration is achieved. Pulling the pipette away from the cell after achieving the whole-cell configuration results in an outside-out patch configuration [24] (Figure 3.1). The on-cell, inside-out, and outside-out modes can give electronic access to, and enables recording of, a single ion channel, whereas the whole-cell mode will give electronic access to all ion channels of the cell, connected in series.

An ion channel switches between being conducting or non-conducting, states which are discrete (Equation 2.6, Figure 3.2). The recording of single-channel currents with patch-clamp will convolute the ligand–receptor on- and off binding-rates with the opening- and closing rates of the ion channel. These rates in a model for ion channel kinetics, can be determined through analysis of the times the channel remain in a conductive and a non-conductive state

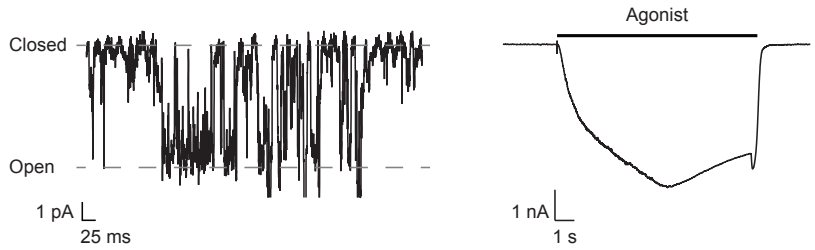

Figure 3.2: Single-channel and whole-cell patch-clamp recordings. (Left) Single-channel recording, the ion channel switches between a closed and an opened state. (Right) Whole-cell recording, a macroscopic current is obtained by the recording of a multitude of ion channels connected in series.

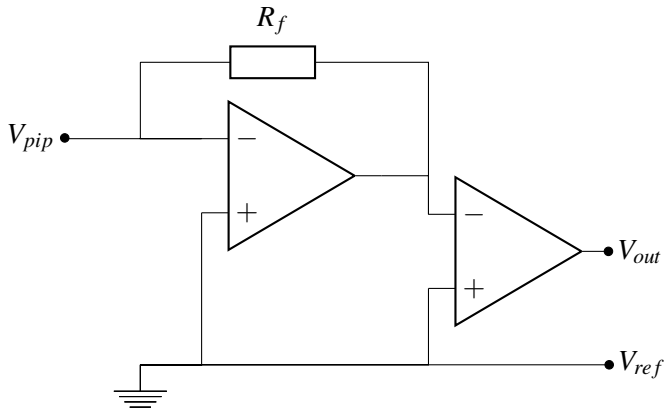

Figure 3.3: Equivalent circuit of a patch-clamp experiment, adapted from Sigworth [119].

[28–32]. Whole-cell recordings involve a large ensemble of ion channels, hence, all the individual openings and closings of ion channels add up to a macrocurrent (Figure 3.2).

3.2 Patch-Clamp Amplifier Feedback Circuitry in Voltage-Clamp Mode

In essence, a patch-clamp amplifier is a very sensitive current-to-voltage converter, able to convert picoampere currents into voltage signals, which readily can be sampled by a computer. In voltage-clamp mode, the pipette potential V_{pip} is maintained constant and equal to the reference potential V_{ref} by an operational amplifier, which is used to measure and adjust V_{pip} via a resistor R_f, i.e. automatic injection of current adjust for the difference between V_{pip} and V_{ref}. The injected current is proportional to the current mediated by the ion-channels gated by a ligand. [119] (Figure 3.3).

3.3 Data Acquisition

According to the Nyquist sampling theorem, the sampling rate should be faster than twice the highest frequency-component within a signal [120, 121]. Low-pass filtering of an electrophysiological signal is therefore necessary to minimize the risk of aliasing the signal, and also reduces background noise, which improves the signal-to-noise ratio. Most often, a low-pass Bessel filter is applied, which is of beneficial use in the time domain, since it causes minimal overshoot of the output signal, if the input is a step function.

4 Microfluidics for Superfusion

> Motion at low Reynolds number is very majestic, slow, and regular.
>
> *(Edward Mills Purcell)*

Microfluidics consider the manipulation of fluids in channels with dimensions in the range of 1–1000 μm, require only small volumes of samples and reagents, and produce little waste [122–125]. In this thesis, microfluidics has been used for superfusion, enabling rapid and precise solution exchange around a cell for the study of ligand-mediated responses. The behaviour of fluids at this scale, where the Reynolds number typically is very low, differ fundamentally from their behaviour in the macroscopic world we are used to [126].

4.1 Superfusion

Rapid and controlled superfusion is important in e.g. studies of ligand-receptor interactions in biological cells. Solution exchange over a cell in a dish for patch-clamp measurements has typically been performed with a glass pipette, e.g. with a θ-tube where the inner tube is separated by a glass septum (hence, the orifice resembles a θ) which allow two solutions to be rapidly switched by moving the pipette, or with a multi-barrel system, which is a variant of the θ-tube but with additional solutions [31, 127]. In this work, microfluidic solution switching devices fabricated with soft lithography have been used for patch-clamp experiments, where a low Reynolds number in combination with a sufficiently high Péclet number of adjacent flows in an open volume, allow the chemical environment around a cell to be rapidly exchanged with a multitude of solutions [33, 128–137]. This method is restricted to assays where cells can be lifted up and transported to the channel exits, which is not possible when working with e.g. neurons that must remain in connection with each other to maintain their functionality. In paper I, a microfluidic pipette was developed which provide a recirculation zone within a confined volume which can be used for directed drug delivery to cells *in situ* (Figure 4.1). Further, in paper III a microfluidic flow cell was used to create a stationary phase of immobilized proteoliposomes [138–141], which allowed chemical analysis of membrane proteins to be performed (Figure 4.2).

4.2 Mathematical Models in Fluid Dynamics

Liquid flow and material transport are two phenomena which can be modelled mathematically, this information is valuable for the design and understanding of microfluidic systems.

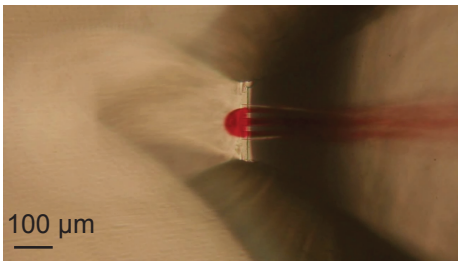

Figure 4.1: The microfluidic pipette described in paper I, which provides recirculation within a confined volume in front of the tip (in red). Image provided by courtesy of Alar Ainla.

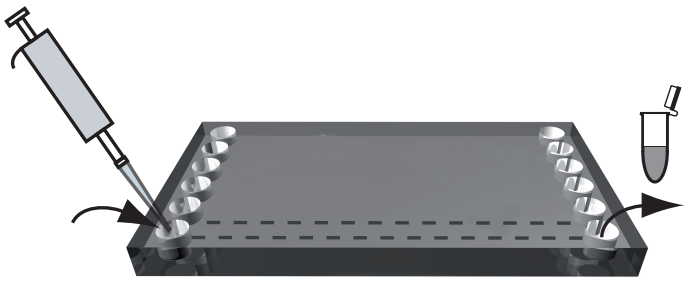

Figure 4.2: Schematic overview of sample handling of immobilized proteoliposomes inside the flow cell channel described in paper III. The flow cell is operated with automatic pipettes, but ferrules can also be fitted into the inlets and outlets to connect e.g. a syringe-pump to the flow cell.

4.2.1 Fluid Motion

The motion of fluids can be described by the Navier-Stokes equations, the form for an incompressible homogeneous Newtonian fluid is

$$\rho\left(\frac{\partial \mathbf{v}}{\partial t}+\mathbf{v}\cdot\nabla\mathbf{v}\right)=-\nabla p+\mu\nabla^2\mathbf{v}+\mathbf{F}_{\mathbf{ext}}, \tag{4.1}$$

where $\mathbf{v}$ is the flow velocity, ρ is the density, p is the pressure, μ is the dynamic viscosity, and $\mathbf{F}_{\mathbf{ext}}$ is the representation of external forces acting on the fluid.

Equation 4.1 is an application of Newton's second law,

$$m\mathbf{a}=\mathbf{F}, \tag{4.2}$$

on fluid motion; the left-hand terms of the equations are inertial, and the right-hand terms are the sum of forces acting on an object (compare Equations 4.1 and 4.2).

The Reynolds number for flow in a channel is defined as the ratio of inertial to viscous forces,

$$Re=\frac{\rho v D_h}{\mu}, \tag{4.3}$$

where v is the characteristic velocity, μ is the viscosity of the liquid, and D_h is the hydraulic diameter, which depends on the geometry of the channel.

If the Reynolds number is small, and the flow is stationary, the inertial terms in the Navier-Stokes equation are neglected. The equation describing the flow profile then becomes

$$\nabla p=\mu\nabla^2\mathbf{v}, \qquad \nabla\cdot\mathbf{v}=0, \tag{4.4}$$

which has a parabolic solution when solved for $\mathbf{v}$ in a system with parallel and infinite plates as in paper III. Given the solution for $\mathbf{v}$ at certain coordinates, the shear force acting on proteoliposomes immobilized on a surface can be calculated [142].

4.2.2 Convection and Diffusion

A molecule in a moving liquid will diffuse while being transported by the flow. This behaviour is described by the convection–diffusion equation,

$$\frac{\partial c}{\partial t}=D\nabla^2 c-\bar{v}\nabla c, \tag{4.5}$$

where c is the concentration, D is the diffusion coefficient, $\bar{v}$ is the average velocity of the flow and t is time.

The Péclet number is defined as the ratio of convection to diffusion,

$$Pe=\frac{vW}{D}, \tag{4.6}$$

where W is the width of the channel, and D is the mass diffusion constant. The Péclet number is e.g. an indicator of how fast a liquid needs to flow, to overcome diffusion.

4.3 Soft Lithography

Microfluidic devices are constructed by molding an inverted pattern into an elastomer, e.g. poly(dimethylsiloxane) (PDMS). PDMS is flexible, transparent, and only slightly permeable to water, and can be bonded to glass by treatment with oxygen plasma [124, 143]. The microfluidic pipette introduced in paper I is made by PDMS, where three channels placed next to each other are used to create a recirculation zone within another liquid. It was made by replica moulding in PDMS, where a master pattern was prepared with photolithography. Then, PDMS was cast on the master, cured, and peeled off from the master. The final device was prepared by bonding different layers of PDMS and glass by treatment with oxygen plasma (Figure 4.3).

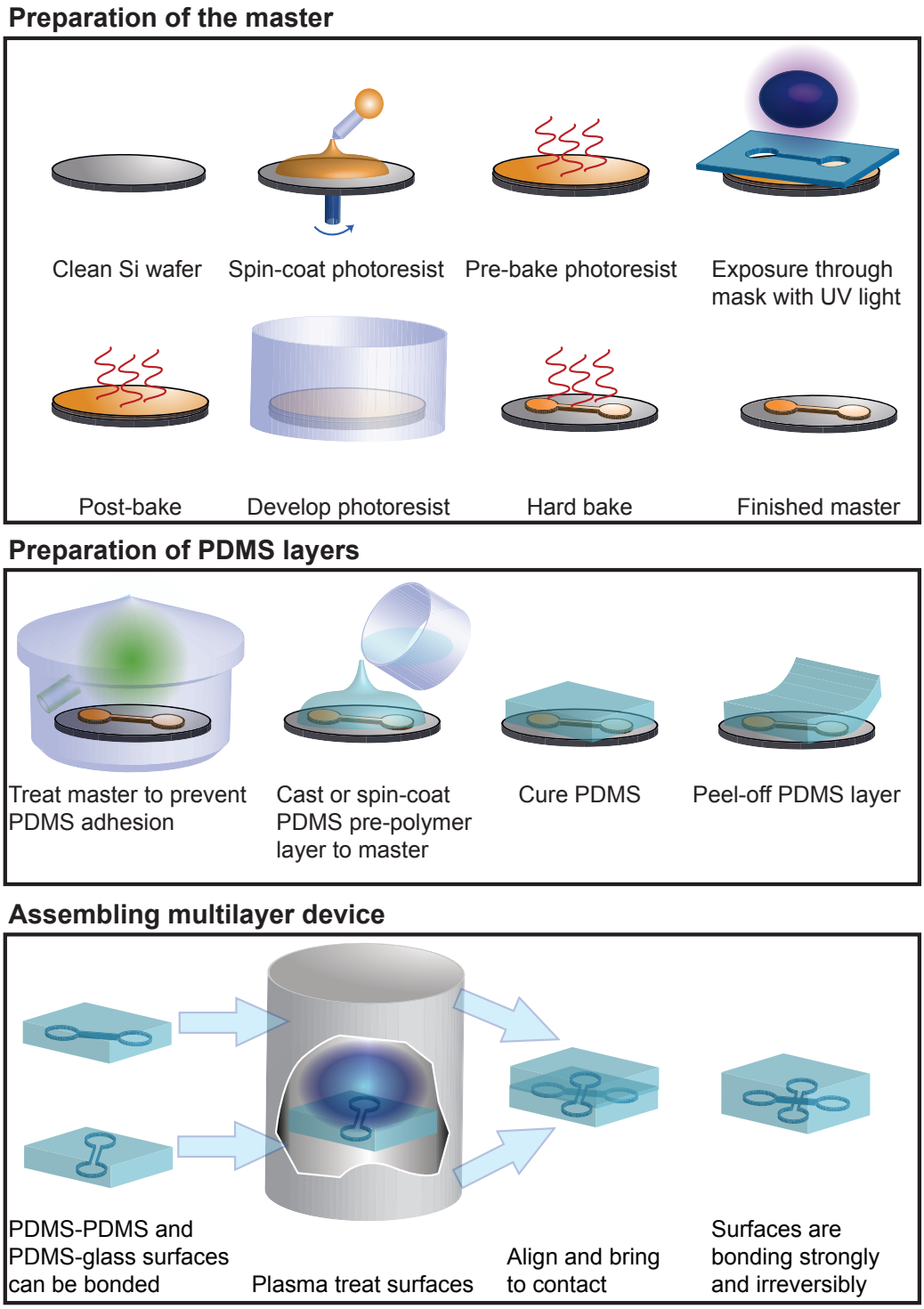

Figure 4.3: Schematic overview of microfabrication with PDMS. Illustration provided by courtesy of Alar Ainla.

5 Imaging

> By the means of Telescopes, there is nothing so far distant but may be represented to our view; and by the help of Microscopes, there is nothing so small as to escape our inquiry; hence there is a new visible World discovered to the understanding.
>
> *(Robert Hooke)*

Imaging with microscopes is a fundamental method, without which many techniques for biological studies would be impossible to perform. Microscopy can be used both as an aid for experimental setup, e.g. as in the case of patch-clamping, or for direct measurements.

5.1 Fluorescence

A molecule can be electronically excited by the absorption of a photon with energy

$$E = hc/\lambda, \tag{5.1}$$

where h is Planck's constant, c is the speed of light, and λ the wavelength of the photon. The absorbance is calculated as

$$A = \log \frac{I_0}{I}, \tag{5.2}$$

where I_0 is the incident light intensity, and I the light intensity transmitted through the sample. The absorbance is also according to the Beer–Lambert law calculated as

$$A = \varepsilon cl, \tag{5.3}$$

where ε is the molar extinction coefficient, c is the concentration, and l is the sample path-length.

After absorption of a photon, a molecule is excited from its singlet ground state to a higher singlet state, e.g. $S_0 \rightarrow S_1$. When returning to its ground state S_0, the molecule can rapidly emit the absorbed energy in the form of a photon, with a wavelength higher than that of the absorbed photon. This is due to the Stokes shift, which often mainly occurs by vibrational relaxation (VR) [144]. The molecule can also transit from the excited singlet state to a another singlet state through internal conversion (IC), e.g. $S_1 \rightarrow S_0$, or to a triplet state via intersystem

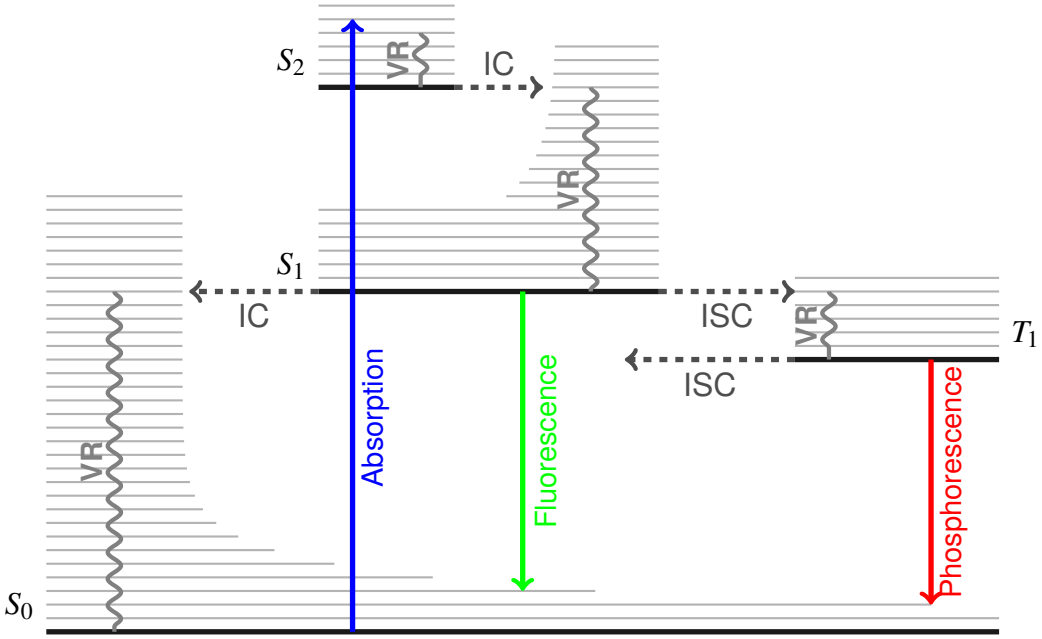

Figure 5.1: A Jabłoński diagram depicting different state transitions which can occur in a fluorophore upon absorption. In the figure, S_n and T_n are the electronic singlet and triplet-states, respectively. Illustration provided by courtesy of Dr. Germain Salvato-Vallverdu.

crossing (ISC), e.g. $S_1 \rightarrow T_1$, these transitions are radiationless [145]. Hence, the efficiency of fluorescence is described by the quantum yield, defined as the ratio of emitted photons to absorbed photons,

$$\phi_f = \frac{k_f}{\sum_i k_i}, \tag{5.4}$$

where k_f is the rate constant for fluorescence emission, and $\sum_i k_i$ is the sum of all rates for decay from the excited state.

The transition from the excited triplet state to the singlet ground state can also occur through the release of a photon. Since this transition, known as phosphorescence, i.e. $T_1 \rightarrow S_0$, is spin forbidden, the rate of this transition is much slower compared to fluorescence [146] (Figure 5.1).

Fluorescent dyes can be used for studying molecular interactions, i.e. fluorescent probes, which have molecular specificity along with spectroscopic properties, allowing for molecularly targeted visualization. A few examples are; Fura-2, a calcium-binding dye which can be used for ratiomeric determination of calcium, and YO-PRO, a dye which quantum yield is drastically increased when bound to DNA [147–149]. Uptake of these probes into biological cells can be mediated e.g. by direct permeability, ion channels, whole-cell patch-clamp pipette delivery, or utilization of membrane permeant ester-forms of the dye [147].

5.2 Optical Resolution

The optical resolution of an microscope, i.e. the limit of how small objects can be and still be separable from each other, is determined by the Rayleigh criterion,

$$R = 0.61\frac{\lambda}{\mathrm{NA}}, \tag{5.5}$$

where NA is the numerical aperture, which describe the range of angles the system can accept or emit light. The numerical aperture in e.g. an objective lens is defined as

$$\mathrm{NA} = n\sin\theta, \tag{5.6}$$

where n is the refractive index of the medium between the objective and the studied object, and θ is the half-angle of the maximum cone of light that can enter or exit the objective. Values of n for mediums the objective typically is working in are 1.0 for air, 1.33 for water, and 1.56 for oils. By using light within the visible spectrum (λ =500 nm) in combination with water as medium between the objective and sample, a resolution of maximum 230 nm can be obtained.

5.3 Laser Scanning Confocal Microscopy

Confocal microscopy differ from conventional light microscopy by limiting the field of illumination and the field of view with apertures, i.e. pinholes. The object of interest is laterally scanned using a point laser source and a point detector. The resulting intensity values are mapped together to form an image. With confocal microscopy, light scattered from parts of the object not currently being illuminated, i.e. out-of-focus light, is rejected, resulting in optical sectioning [150–152]. A photomultiplier tube is commonly used as a detector which collects the light passing the pinhole, and converts the photons into an intensity value of a pixel (Figure 5.2). The thin optical sectioning enabled by the use of a pinhole makes imaging of different planes in a sample possible, hence a three-dimensional image of the object can be obtained. The technique is minimally non-invasive, and imaging of live cells can readily be performed, e.g. after treatment with fluorescent dyes, or if the cells express fluorescent molecules (Figure 5.3).

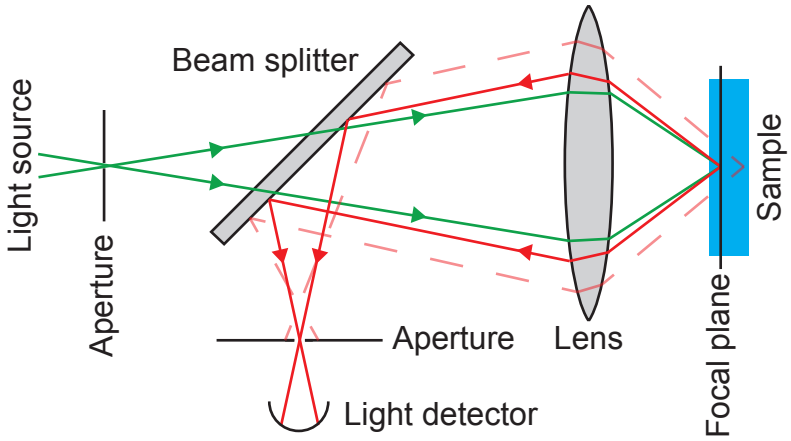

Figure 5.2: Schematic overview of beam pathway in a confocal microscope. Only light from the focal plane can pass through the pinhole and reach the detector, whereas unfocused light from other planes of the sample is scattered on the aperture wall.

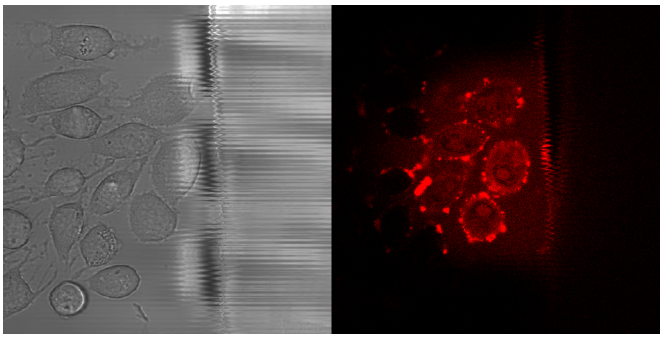

Figure 5.3: Cellular YO-PRO uptake induced by stimulation of TRPV1 with capsaicin, the microfluidic pipette described in paper I is used for drug delivery. (Left) Transmission image. (Right) Fluorescence image.

6 Proteomics

> Das Kathodenlicht der Entladung des Inductoriums durch verdünnte Gase besteht aus mehreren verschieden gefärbten Schichten.
>
> *(Eugen Goldstein)*

Proteomics consider analysis of the types and levels of proteins expressed in a cell, a field supplementary to genomics which consider studies of the genome [153–156]. Proteins can be identified by the use of mass spectrometry (MS), a flexible tool which can be used for proteomic top-down and bottom-up analysis. While the post-translational modifications of single proteins can be readily studied with the top-down approach, protein identifications in high-complexity samples is handled by the bottom-up approach [13–18]. For the identification of proteins with bottom-up proteomics, all proteins in a mixture are digested into peptides by a protease. The resulting peptides are then separated by one- or multidimensional liquid chromatography (LC), followed by analysis with tandem mass spectrometry (MS/MS). The complex spectral data set resulting as output from this analysis is most often searched and compared against a protein database, in order to obtain a list of proteins found in the sample [16, 157–160]. Mass spectrometry can also be used to probe protein interactions [161].

6.1 Peptide Sequencing

Determination of the ordered peptide sequence of a protein has for a long time been performed by Edman degradation [162], for which automated methods exist and relies on stepwise chemical cleavage from the N-terminal. However, development of MS-techniques and computational power, displaced Edman degradation as a method for peptide sequencing, as MS can fragment peptides in milliseconds instead of hours or days [160].

For peptide analysis with MS, proteins are first degraded into peptides using a protease, e.g. trypsin, which specifically cleaves a protein (or peptide) at the carboxylic side of arginine and lysine. The resulting peptides are injected onto a nano LC-column coupled to an MS, where the peptides are chromatographically separated based on their polarity [160].

For MS-detection, the peptides need to be ionized, which can be performed by electrospray ionization (ESI), which can be connected online to an LC-system. Ionization can also be achieved with matrix-assisted laser desorption/ionization (MALDI), but this technique can however not be directly coupled to an LC-system. For their work on these techniques, Koichi Tanaka and John Fenn were awarded with the Nobel prize in chemistry in 2002. In order to determine the structure of the peptide of interest, it must undergo fragmentation, which is most

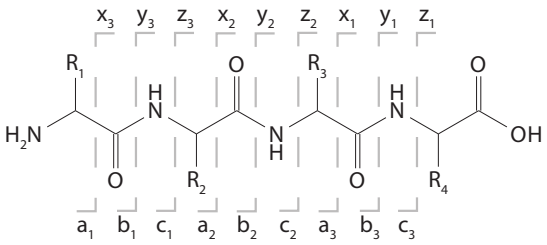

Figure 6.1: Fragmentation of peptides according to Roepstorff–Fohlmann–Biemann nomenclature. Adapted from Watson and Sparkman [156].

often performed by collision-induced dissociation (CID). In MS/MS, the ion to be fragmented is selected (data-dependently) by the first mass analyser, and is sent on to a collision cell, where the ion collides with uncharged gas atoms, causing dissociation of the ion. With high-energy CID, all fragments in Figure 6.1 can be found, together with further possible fragments of the peptide not accounted for herein. Using low-energy CID, mainly *b*- and *y*-ions are formed. The resulting fragments are then analysed by a second mass analyser, which gives the mass spectrum of the peptide. The mass analyser measures the mass-to-charge ratio, m/z, of an ion, rather than the mass itself. There exist many different types of mass analysers, where a recent invention is the orbitrap, in which ions are trapped in orbitals by an electrostatic field. The oscillation frequency of the ions is linked to the mass-to-charge ratio, and a fast Fourier transformation algorithm is used to convert the time-domain signal into a mass-to-charge spectrum. The orbitrap is most often used in combination with a linear ion trap, where the orbitrap would acquire full MS scans while the linear ion trap would detect the fragmentation ions after CID. [18, 156, 163, 164]. The mass differences between consecutive ions in a series, in combination with fragmentation patterns, allows the amino acid sequence of the peptide to be determined (Table 6.1).

6.2 Protein Identification

Protein identification is achieved by comparing data obtained from MS/MS with those predicted for all the proteins in a database, i.e. the mass profiles of peptides obtained from digested proteins in experimental measurements are compared, using a computer program, with theoretical MS/MS profiles of all predicted peptides. The method can readily be applied to very complex mixtures of proteins, where also a dynamic exclusion filter can be set in the MS instrument method to achieve maximal detection of unique peptides. Various algorithms exist for the purpose of database search and identification, called peptide fragmentation fingerprinting, e.g. SEQUEST and MASCOT [163]. The information on partial peptide sequence obtained with MS/MS allows two peptides with identical amino acid content but with different sequences to be separated from each other, as their fragmentation pattern will differ. A requirement of this method is that the protein of interest already exists in a database, if it is not present, the gene encoding the proteins needs to be cloned and sequenced. Usually, to limit

Table 6.1: Mass increments of amino acids. Adapted from de Hoffmann and Stroobant [163] and Watson and Sparkman [156].

Amino acid	Code (3 letters)	Code (1 letter)	Monoisotopic mass	Chemical mass
Glycine	Gly	G	57.02147	57.052
Alanine	Ala	A	71.03712	71.079
Serine	Ser	S	87.03203	87.078
Proline	Pro	P	97.05277	97.117
Valine	Val	V	99.06842	99.133
Threonine	Thr	T	101.04768	101.105
Cysteine	Cys	C	103.00919	103.144
Isoleucine	Ile	I	113.08407	113.160
Leucine	Leu	L	113.08407	113.160
Asparagine	Asn	N	114.04293	114.104
Aspartate	Asp	D	115.02695	115.089
Glutamine	Gln	Q	128.05858	128.131
Lysine	Lys	K	128.09497	128.174
Glutamate	Glu	E	129.04260	129.116
Methionine	Met	M	131.04049	131.198
Histidine	His	H	137.05891	137.142
Phenylalanine	Phe	F	147.06842	147.177
Arginine	Arg	R	156.10112	156.188
Tyrosine	Tyr	Y	163.06333	163.176
Tryptophan	Trp	W	186.07932	186.213

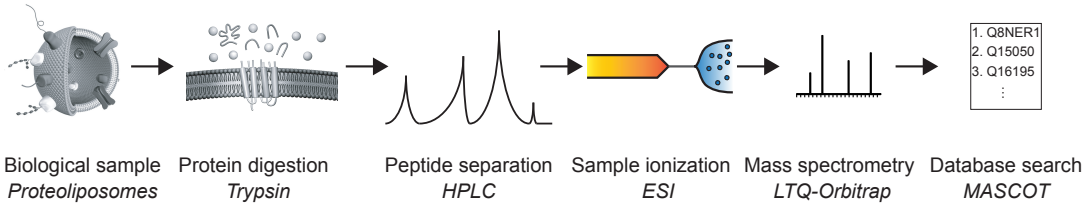

Figure 6.2: Schematic overview of bottom-up proteomic analysis using LC–MS/MS. Proteins obtained from a biological sample are digested by a protease, the resulting peptides are analyzed by LC–MS/MS, and the data obtained is searched against a database whereby the proteins can be identified. Adapted from Steen and Mann [160].

false positives in protein identification, the experimental data is also searched and compared against a reversed database, i.e. a database where the predicted peptide sequences have been inverted, hence containing non-sense data [165–167]. A threshold value is set, determining the false discovery rate considered to be acceptable. Finally, the database search output delivers a list of identified proteins, how many peptides that have been uniquely associated with a protein, and a confidence score on how reliable the identification is (Figure 6.2).

6.3 Limited Proteolysis

Only a small fraction of membrane proteins expressed in mammalian hosts have a structure determined from X-ray crystallography [11], as crystallization of membrane proteins is an complicated issue. Limited proteolysis can be used for probing flexible regions of the three-dimensional structure of a protein while still residing in its native lipid environment [19, 168]. The technique is performed by limiting the activity of a protease, by control of e.g. temperature, protease concentrations and digestion time. By restricting the protease, its activity will mainly digest flexible regions, and partnered with MS, the detection and localization of the resulting peptides can be used for structural analysis [12, 169].

6.4 Proteoliposomes

The preparation of proteoliposomes derived from cultured cells decreases the biological complexity of a cell, yet the membrane proteins are still residing in, or associated with the cellular lipid bilayer. Proteoliposomes can be prepared in various ways, e.g. by blebbing [170–173] or by reconstitution of membrane proteins into artificial liposomes [174]. Here, proteoliposomes were prepared by lysis and mechanical disruption of cultured cells with a Dounce homogenizer [175], in combination with ultracentrifugation and sonication (Figure 6.3).

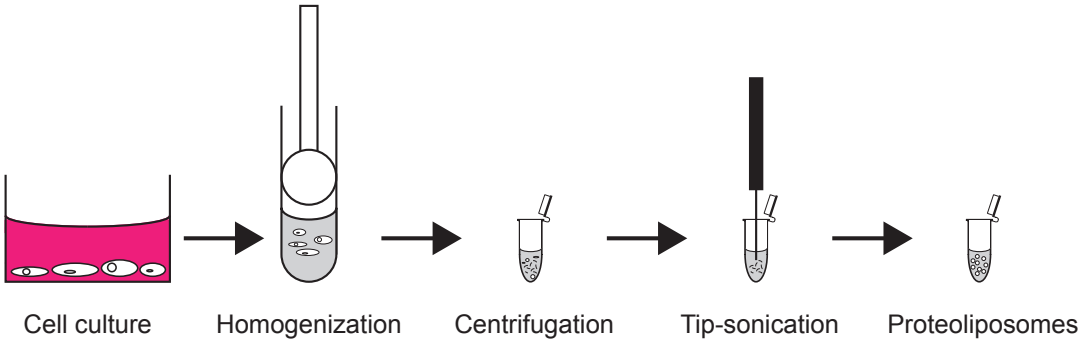

Figure 6.3: Schematic overview of preparation of proteoliposomes cultured cells. Cells are cultured, harvested, and then lysed by osmotic pressure in combination with mechanical disruption. The cell lysate is centrifuged to remove nuclei and mitochondria. The remaining membrane fraction is tip-sonicated, which results in the formation of proteoliposomes.

7 Summary of Results

> Vår tid är i främsta rummet en praktisk tid. Den kräver av oss alla i vårt arbete klara, påtagliga resultat. Det är därför endast naturligt, att även den rent vetenskapligt inriktade forskaren understundom ställer sig den frågan: kan någon nytta komma av min forskning och mitt arbete?
>
> *(The Svedberg)*

The papers included in this thesis present results from the development of methods for membrane protein analysis, along with characterization of the ion channel TRPV1, which is involved in human nociception. Both structure and function of membrane proteins have been investigated, as well as the interconnection between these protein characteristics. Paper I and III describe the developed methods and evaluate them, and paper II and IV consider investigations of chemical modulation of TRPV1, where the methods from the previous papers have been applied.

7.1 Paper I

A microfluidic pipette made of poly(dimethylsiloxane) was developed, where a recirculation of liquid is obtained by varying the pressures of the three channels in the pipette, which generates a confined volume zone in front of the pipette (Figure 7.1). The pipette is capable of performing various complex fluid processing operations, e.g. mixing, multiplexing, or gradient generation, and switching between solutions is rapid (<100 ms). Ion channel function was measured by uptake of the fluorescent dye YO-PRO in Chinese hamster ovary (CHO) cells expressing TRPV1, in an experiment where the microfluidic pipette was used for superfusion of cells with agonist, showing it being capable of generating a dose-response curve. We also activated TRPV1 in single cells and measured responses with whole-cell patch-clamp, and induced membrane bleb formation by exposing selected groups of cells to formaldehyde/dithiothreitol using the pipette as a drug delivery system. The microfluidic pipette enables studies on adherent cells which can not be moved, e.g. neuronal cells, as the perfusion zone can be placed at an arbitrary point in a cell culture dish, and provides contamination-free multiple-compound delivery for pharmacological screening.

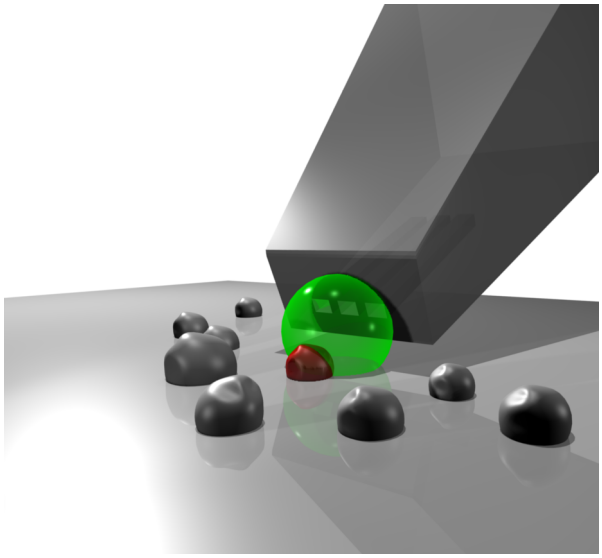

Figure 7.1: Schematic illustration of the microfluidic pipette in paper I, targeting a single cell (red) for drug delivery with a confined recirculation zone (green) which leaves cells not in contact with the boundary of the circulation zone unaffected (grey).

7.2 Paper II

The effect of cholesterol depletion on TRPV1 pore dilation was investigated by measuring ion channel permeability with whole-cell patch-clamp and fluorescence studies in CHO cells expressing TRPV1, utilizing microfluidic devices, e.g. the pipette developed in Paper I. Depletion of cholesterol was found to impair the dynamic permeability of large cations in TRPV1. During sustained activation with capsaicin and under hypocalcemic conditions, the permeability of the large cation N-methyl-D-glucamine (NMDG) increases over time in control cells. This process was found to be inhibited in cells where cholesterol was depleted, as the relative permeability of NMDG to Na^+ was decreased by 70% upon cholesterol depletion compared to control cells. Also, the uptake rate of the cationic fluorescent dye YO-PRO during sustained activation with capsaicin under hypocalcemic conditions, was decreased by 50% in cholesterol-depleted cells compared to control cells (Figure 7.2). A decrease in permeability for large cations was also observed in cholesterol-depleted cells when TRPV1 was activated with protons (pH 5.5). We found the level of cholesterol depletion necessary for inhibition of dynamic permeability to be dependent on type of agonist, as a decrease of cholesterol content by 36% was sufficient to inhibit this process when activating TRPV1 with 1 µM capsaicin, but not with protons (pH 5.5) as an agonist, where the latter required a cholesterol depletion of 54% to achieve an inhibitory effect of the time-dependent permeability. These results propose a novel mechanism by which cellular cholesterol-depletion modulates the function of TRPV1, which may constitute a novel pharmacological approach for treatment of neurogenic pain.

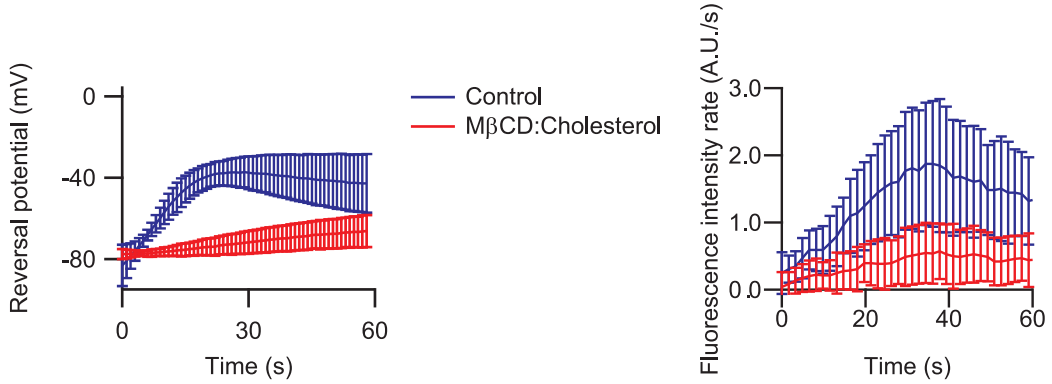

Figure 7.2: Changes in dynamic permeability of TRPV1 for large cations were inhibited by cholesterol depletion with cyclodextrins in paper II. (Left) The change in reversal potential with external NMDG upon sustained activation with capsaicin was inhibited with cholesterol depletion. (Right) The uptake rate of YO-PRO was decreased in cholesterol-depleted cells upon sustained activation of TRPV1 with protons (pH 5.5).

7.3 Paper III

A microfluidic flow cell for immobilization of proteoliposomes was developed, enabling flexible chemistry to be performed on membrane proteins. Utilizing the stationary phase of proteoliposomes, a sequential tryptic digestion protocol for proteomic characterization was developed, where the peptides resulting from stepwise enzymatic digestion of the proteoliposomes was analyzed with LC–MS/MS (Figure 7.3). The flow cell is assembled by mounting two parallel gold surfaces face to face, separated by a thin spacer, and feature an inlet and an outlet port. Proteoliposomes were obtained from red blood cells and CHO cells, which were found to immobilize on the inside of the flow cell channel. The rate of proteoliposome immobilization was determined with quartz crystal microbalance with dissipation monitoring (QCM-D), which showed 95% of the proteoliposomes to bind the surface within 5 min. The flow cell was found to have a binding capacity of 1 µg proteoliposomes/cm^2, hence, a proteoliposome-concentration of 500 µg/ml is required to achieve saturation of the flow cell channel surfaces. Imaging with atomic force microscopy showed an even distribution of the proteoliposomes upon immobilization. A hydrodynamic analysis was performed, which determined the force acting on the proteoliposomes during flow cell operation to be in the range of 0.1–1 pN, too small to cause any deformation or rupture of proteoliposomes. The sequential digestion protocol was found to detect 65% more unique membrane-associated protein compared to a single-digest protocol, proving it as a suitable tool for shotgun proteomics on proteoliposomes, as it enables more detailed characterization of complex protein samples.

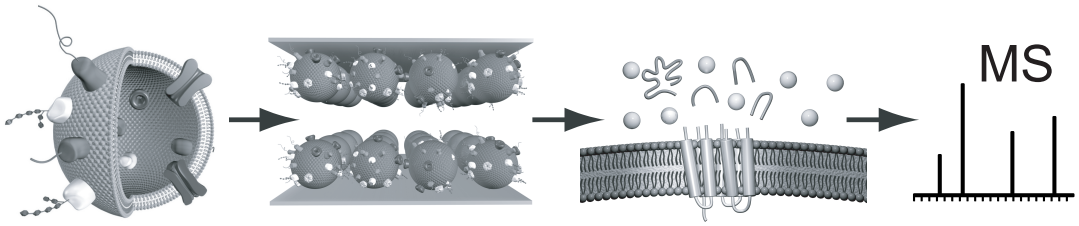

Figure 7.3: Schematic overview of the workflow for peptide analysis in paper III. Proteoliposomes are immobilized in the flow cell channel, whereafter proteins of the proteoliposomes are digested with a protease. The resulting peptides are analyzed with LC–MS/MS.

7.4 Paper IV

Many hereditary diseases involve malfunctioning ion channels, where more knowledge regarding their structure and function could be an important aid for drug development. Structural information of membrane proteins can be hard to obtain with many techniques, due to their partly hydrophobic nature. Here, the topology of TRPV1 was probed by limited sequential digestion of immobilized proteoliposomes, described in paper III, where the peptides were identified with LC–MS/MS (Figure 7.4). The proteoliposomes prepared for proteomic analysis were found to carry functional TRPV1, as calcium release from immobilized proteoliposomes was observed with the fluorescent dye Fura-2 in the flow cell channel, upon stimulation with capsaicin. After the identification of flexible regions of the protein upon time- and concentration-limited digestion with trypsin, the effect of TRPV1-truncation on its activity was studied. This was achieved by performing limited proteolysis on TRPV1 located in immobilized proteoliposomes in the flow cell channel, followed by stimulation with capsaicin and observation of calcium release with Fura-2. Limited proteolysis was also performed in combination with patch-clamp measurements of TRPV1 in the inside-out recording mode, by recording ion channel currents upon stimulation with capsaicin, followed by tryptic digestion of the N- and C-terminals, and thereafter recording currents again during stimulation with capsaicin. With chemical truncation of TRPV1 *in situ*, we identified peptide regions of the ion channel without which it was still possible for capsaicin to bind to and activate TRPV1.

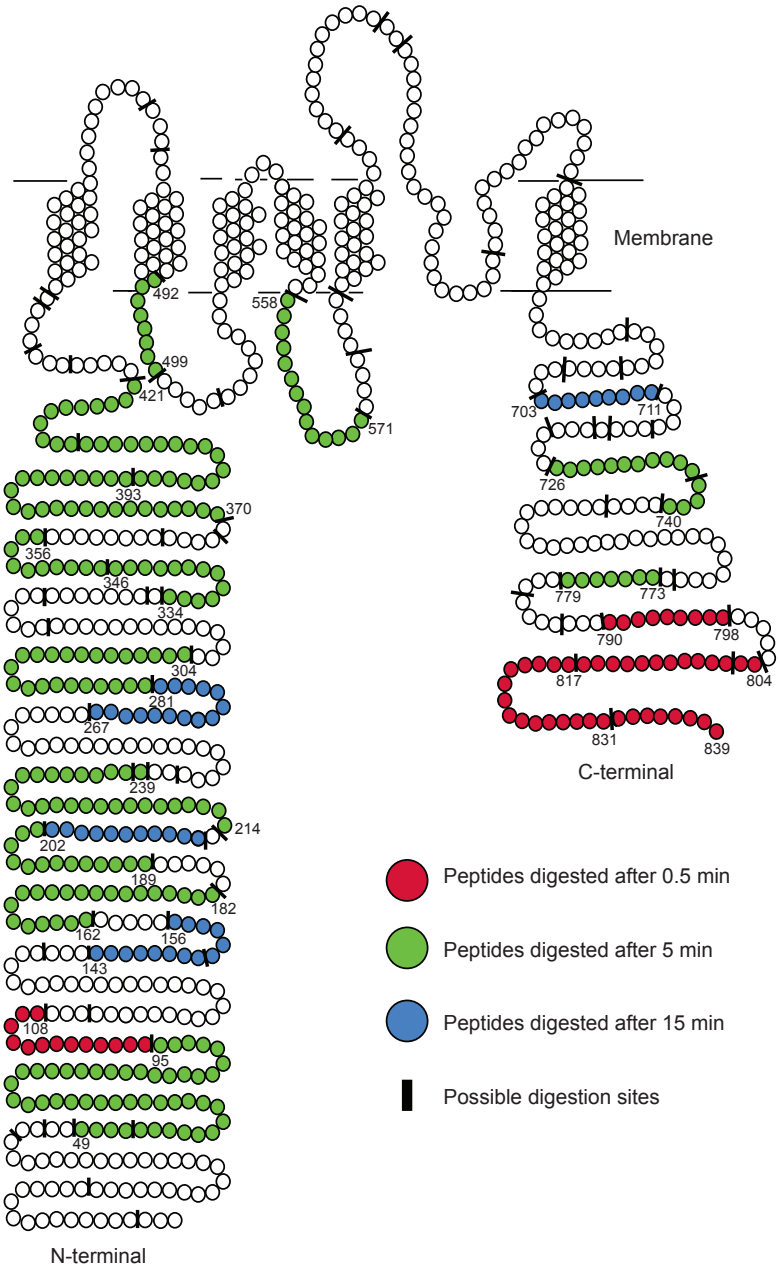

Figure 7.4: Peptides detected after sequential digestion of TRPV1-proteoliposomes in paper IV. Colour encoding denote time of cumulative tryptic digestion before detection with LC–MS/MS.

8 Concluding Remarks

> Om jag får 300 idéer på ett år och en är användbar, då är jag nöjd.
>
> *(Alfred Nobel)*

The herein developed methods for analysis of membrane proteins have been evaluated and established as functional concepts, which may constitute tools in studies of basic structure–functions interconnections of proteins as well as in drug development. The miniaturization which follows the fabrication of microfluidic devices reduces the amount of biological sample and chemicals necessary for analysis. The versatility of chemical delivery provided by these devices, make them applicable in many different settings of protein studies. Concerning the microfluidic pipette, further development is already ongoing, e.g. a modification of the pipette which makes it suitable for *in vivo* drug delivery, which require fabrication in stiffer materials than PDMS and further miniaturization.

Regarding the ion channel studies performed herein, the effect of membrane composition on TRPV1 functionality is a finding which gives another piece to the puzzle of ion channel dynamics and their regulation. It is likely that more exploratory work on the theme of membrane fluidics and ion channel activity would yield further interesting observations if studied *in vivo*, e.g. how regulation of membrane sterol content may effect pain.

Studies of the structure–function relationship of ion channels are usually conducted with the aid of molecular biology techniques, where mutations are induced in the DNA encoding the protein, followed by its expression and analysis. Here, combining patch-clamp and fluorescence measurements with proteomic analysis, connected by limited proteolysis, we have provided a fast shotgun method for chemical truncation of a membrane protein *in situ*, which allows the impact on function of various peptide regions in an ion channel to be assessed. Also, the topological mapping of membrane proteins with proteases followed by peptide detection with mass spectrometry is by itself providing important information, as it yields experimental data which can be used to verify computational predictions of membrane protein structure.

The meeting of technology and science, e.g. the development of experimental methods, which provide new possibilities in biological investigations, in concert with the aim of understanding membrane protein function, is a prolific concept in general which hopefully will continue to provide further understanding of the complex nature of the biological cell.

Acknowledgements

I thank the following people who in various ways have supported the writing of this thesis:

- Professor Owe Orwar, for giving me the opportunity to work on this project and for being an excellent supervisor. Your genuine curiosity in science has been a vast source for inspiration.
- Professors Aldo Jesorka and Kent Jardemark, for outstanding laboratory supervision.
- Professor Per Lincoln, for fruitful discussions of molecular interactions, mathematics and classical music.
- Dr. Gavin D. M. Jeffries, for superior aid in microscopy and imaging, and general techsaviness.
- İrep, for enduring to have me as an office mate. Not many have succeeded with that challenge. It has been a hilarious time.
- Alar, for being a great travel company at conferences and for always taking his time.
- Maria, Carolina, and Akram, the ion channel team, for all the work in patch-clamp land.
- Max, Anders and Roger, for your support in vesicle-business and discussions on body metabolism.
- Previous and present people in the research group and at the division of Physical Chemistry.
- All my friends and relatives for being around.
- Lars, Kristina, KJ and Rikard for their presence in my life.
- My parents for their love and never-ending support of my undertakings.
- Louise, Theodor and Joanna. I love you so much.

Bibliography

[1] Haga, K., Kruse, A. C., Asada, H., Yurugi-Kobayashi, T., Shiroishi, M., Zhang, C., Weis, W. I., Okada, T., Kobilka, B. K., Haga, T., and Kobayashi, T. (2012) Structure of the human M2 muscarinic acetylcholine receptor bound to an antagonist. *Nature 482*, 547–551.

[2] Jentsch, T. J., Steinmeyer, K., and Schwarz, G. (1990) Primary structure of *Torpedo marmorata* chloride channel isolated by expression cloning in *Xenopus* oocytes. *Nature 348*, 510–514.

[3] Doyle, D. A., Morais Cabral, J., Pfuetzner, R. A., Kuo, A., Gulbis, J. M., Cohen, S. L., Chait, B. T., and MacKinnon, R. (1998) The structure of the potassium channel: molecular basis of K^+ conduction and selectivity. *Science 280*, 69–77.

[4] Lundstrom, K. (2006) Structural genomics for membrane proteins. *Cell. Mol. Life Sci. 63*, 2597–2607.

[5] Scheraga, H. A., Khalili, M., and Liwo, A. (2007) Protein-folding dynamics: overview of molecular simulation techniques. *Annu. Rev. Phys. Chem. 58*, 57–83.

[6] Zhang, Y. (2008) Progress and challenges in protein structure prediction. *Curr. Opin. Struct. Biol. 18*, 342–348.

[7] Long, S. B., Campbell, E. B., and MacKinnon, R. (2005) Crystal structure of a mammalian voltage-dependent Shaker family K^+ channel. *Science 309*, 897–903.

[8] Montaville, P., and Jamin, N. In *Membrane protein structure determination: methods and protocols*; Lacapère, J.-J., Ed.; Methods in Molecular Biology; Springer, 2010; Vol. 654; Chapter 14: Determination of membrane protein structures using solution and solid-state NMR., pp 261–282.

[9] Bokoch, M. P. et al. (2010) Ligand-specific regulation of the extracellular surface of a G-protein-coupled receptor. *Nature 463*, 108–112.

[10] Granier, S., and Kobilka, B. (2012) A new era of GPCR structural and chemical biology. *Nat. Chem. Biol. 8*, 670–673.

[11] Bill, R. M., Henderson, P. J. F., Iwata, S., Kunji, E. R. S., Michel, H., Neutze, R., Newstead, S., Poolman, B., Tate, C. G., and Vogel, H. (2011) Overcoming barriers to membrane protein structure determination. *Nat. Biotechnol. 29*, 335–340.

[12] Hyung, S.-J., and Ruotolo, B. T. (2012) Integrating mass spectrometry of intact protein complexes into structural proteomics. *Proteomics 12*, 1547–1564.

[13] Mann, M., and Wilm, M. (1994) Error-tolerant identification of peptides in sequence databases by peptide sequence tags. *Anal. Chem. 66*, 4390–4399.

[14] Peng, J., and Gygi, S. P. (2001) Proteomics: the move to mixtures. *J. Mass Spectrom. 36*, 1083–1091.

[15] Han, X., Jin, M., Breuker, K., and McLafferty, F. W. (2006) Extending top-down mass spectrometry to proteins with masses greater than 200 kilodaltons. *Science 314*, 109–112.

[16] Dowell, J. A., Frost, D. C., Zhang, J., and Li, L. (2008) Comparison of two-dimensional fractionation techniques for shotgun proteomics. *Anal. Chem. 80*, 6715–6723.

[17] Tang, J., Gao, M., Deng, C., and Zhang, X. (2008) Recent development of multi-dimensional chromatography strategies in proteome research. *J. Chromatogr. B Analyt. Technol. Biomed. Life Sci. 866*, 123–132.

[18] Yates, J. R., Ruse, C. I., and Nakorchevsky, A. (2009) Proteomics by mass spectrometry: approaches, advances, and applications. *Annu. Rev. Biomed. Eng. 11*, 49–79.

[19] Fontana, A., de Laureto, P. P., Spolaore, B., Frare, E., Picotti, P., and Zambonin, M. (2004) Probing protein structure by limited proteolysis. *Acta Biochim. Pol. 51*, 299–321.

[20] Hübner, C. A., and Jentsch, T. J. (2002) Ion channel diseases. *Hum. Mol. Genet. 11*, 2435–2445.

[21] Ashcroft, F. M. (2006) From molecule to malady. *Nature 440*, 440–447.

[22] Neher, E., and Sakmann, B. (1976) Single-channel currents recorded from membrane of denervated frog muscle fibres. *Nature 260*, 799–802.

[23] Sakmann, B., Patlak, J., and Neher, E. (1980) Single acetylcholine-activated channels show burst-kinetics in presence of desensitizing concentrations of agonist. *Nature 286*, 71–73.

[24] Hamill, O. P., Marty, A., Neher, E., Sakmann, B., and Sigworth, F. J. (1981) Improved patch-clamp techniques for high-resolution current recording from cells and cell-free membrane patches. *Pflugers Arch. 391*, 85–100.

[25] Zhao, Y., Inayat, S., Dikin, D., Singer, J., Ruoff, R., and Troy, J. (2008) Patch clamp technique: Review of the current state of the art and potential contributions from nanoengineering. *Proc. Inst. Mech. Eng. Part N-J. Nanoeng. Nanosyst. 222*, 1–11.

[26] Balasubramanian, B., Imredy, J. P., Kim, D., Penniman, J., Lagrutta, A., and Salata, J. J. (2009) Optimization of Cav1.2 screening with an automated planar patch clamp platform. *J. Pharmacol. Toxicol. Methods 59*, 62 – 72.

[27] Möller, C., and Witchel, H. (2011) Automated electrophysiology makes the pace for cardiac ion channel safety screening. *Front. Pharmacol. 2*, 73.

[28] Colquhoun, D., and Hawkes, A. G. In *Single-channel recording*, 2nd ed.; Sakmann, B., and Neher, E., Eds.; Plenum Press: New York, 1995; Chapter 18: The principles of the stochastic interpretation of ion-channel mechanisms, pp 397–482.

[29] Hatton, C. J., Shelley, C., Brydson, M., Beeson, D., and Colquhoun, D. (2003) Properties of the human muscle nicotinic receptor, and of the slow-channel myasthenic syndrome mutant εL221F, inferred from maximum likelihood fits. *J. Physiol. 547*, 729–760.

[30] Burzomato, V., Beato, M., Groot-Kormelink, P. J., Colquhoun, D., and Sivilotti, L. G. (2004) Single-channel behavior of heteromeric $\alpha 1\beta$ glycine receptors: an attempt to detect a conformational change before the channel opens. *J. Neurosci. 24*, 10924–10940.

[31] Bianchi, M. T., Botzolakis, E. J., Haas, K. F., Fisher, J. L., and Macdonald, R. L. (2007) Microscopic kinetic determinants of macroscopic currents: insights from coupling and uncoupling of $GABA_A$ receptor desensitization and deactivation. *J. Physiol. 584*, 769–787.

[32] Lape, R., Colquhoun, D., and Sivilotti, L. G. (2008) On the nature of partial agonism in the nicotinic receptor superfamily. *Nature 454*, 722–727.

[33] Millingen, M., Bridle, H., Jesorka, A., Lincoln, P., and Orwar, O. (2008) Ligand-specific temperature-dependent shifts in EC_{50} values for the $GABA_A$ receptor. *Anal. Chem. 80*, 340–343.

[34] Crick, F. H. (1958) On protein synthesis. *Symp. Soc. Exp. Biol. 12*, 138–163.

[35] Alberts, B. *Molecular biology of the cell*, 4th ed.; Garland Science: New York, 2002.

[36] Levental, I., Grzybek, M., and Simons, K. (2010) Greasing their way: lipid modifications determine protein association with membrane rafts. *Biochem.-Moscow 49*, 6305–6316.

[37] Pucadyil, T. J., and Chattopadhyay, A. (2004) Cholesterol modulates ligand binding and G-protein coupling to serotonin(1A) receptors from bovine hippocampus. *Biochim. Biophys. Acta 1663*, 188–200.

[38] Morenilla-Palao, C., Pertusa, M., Meseguer, V., Cabedo, H., and Viana, F. (2009) Lipid raft segregation modulates TRPM8 channel activity. *J. Biol. Chem. 284*, 9215–9224.

[39] Chubinskiy-Nadezhdin, V. I., Negulyaev, Y. A., and Morachevskaya, E. A. (2011) Cholesterol depletion-induced inhibition of stretch-activated channels is mediated via actin rearrangement. *Biochem. Biophys. Res. Commun. 412*, 80–85.

[40] Xing, Y., Gu, Y., Xu, L.-C., Siedlecki, C. A., Donahue, H. J., and You, J. (2011) Effects of membrane cholesterol depletion and GPI-anchored protein reduction on osteoblastic mechanotransduction. *J. Cell. Physiol. 226*, 2350–2359.

[41] Brown, D. A., and Rose, J. K. (1992) Sorting of GPI-anchored proteins to glycolipid-enriched membrane subdomains during transport to the apical cell surface. *Cell 68*, 533–544.

[42] Nicolau, D. V., Jr, Burrage, K., Parton, R. G., and Hancock, J. F. (2006) Identifying optimal lipid raft characteristics required to promote nanoscale protein-protein interactions on the plasma membrane. *Mol. Cell. Biol. 26*, 313–323.

[43] Graziani, A., Rosker, C., Kohlwein, S. D., Zhu, M. X., Romanin, C., Sattler, W., Groschner, K., and Poteser, M. (2006) Cellular cholesterol controls TRPC3 function: evidence from a novel dominant-negative knockdown strategy. *Biochem. J. 396*, 147–155.

[44] Owen, D. M., Magenau, A., Williamson, D., and Gaus, K. (2012) The lipid raft hypothesis revisited–new insights on raft composition and function from super-resolution fluorescence microscopy. *Bioessays 34*, 739–747.

[45] Ohtani, Y., Irie, T., Uekama, K., Fukunaga, K., and Pitha, J. (1989) Differential effects of α-, β- and γ-cyclodextrins on human erythrocytes. *Eur. J. Biochem. 186*, 17–22.

[46] Christian, A. E., Haynes, M. P., Phillips, M. C., and Rothblat, G. H. (1997) Use of cyclodextrins for manipulating cellular cholesterol content. *J. Lipid Res. 38*, 2264–2272.

[47] Ishikawa, T. T., MacGee, J., Morrison, J. A., and Glueck, C. J. (1974) Quantitative analysis of cholesterol in 5 to 20 microliter of plasma. *J. Lipid Res. 15*, 286–291.

[48] Klansek, J. J., Yancey, P., Clair, R. W. S., Fischer, R. T., Johnson, W. J., and Glick, J. M. (1995) Cholesterol quantitation by GLC: artifactual formation of short-chain steryl esters. *J. Lipid Res. 36*, 2261–2266.

[49] Amundson, D. M., and Zhou, M. (1999) Fluorometric method for the enzymatic determination of cholesterol. *J. Biochem. Biophys. Methods 38*, 43–52.

[50] Dinh, T., Jr., J. B., Brooks, J., Miller, M., and Thompson, L. (2008) A simplified method for cholesterol determination in meat and meat products. *J. Food Compos. Anal. 21*, 306–314.

[51] Robinet, P., Wang, Z., Hazen, S. L., and Smith, J. D. (2010) A simple and sensitive enzymatic method for cholesterol quantification in macrophages and foam cells. *J. Lipid Res. 51*, 3364–3369.

[52] Hille, B. *Ion channels of excitable membranes*, 3rd ed.; Sinauer Associates: Sunderland, Massachusetts., 2001.

[53] Shannon, R. D., and Prewitt, C. T. (1969) Effective ionic radii in oxides and fluorides. *Acta Crystallogr. B 25*, 925–946.

[54] Shannon, R. D. (1976) Revised effective ionic radii and systematic studies of interatomic distances in halides and chalcogenides. *Acta Crystallogr. A 32*, 751–767.

[55] Hellgren, M., Sandberg, L., and Edholm, O. (2006) A comparison between two prokaryotic potassium channels (KirBac1.1 and KcsA) in a molecular dynamics (MD) simulation study. *Biophys. Chem. 120*, 1–9.

[56] Kandel, E. R., Schwartz, J. H., and Jessell, T. M. *Principles of neural science*, 4th ed.; McGraw-Hill: New York, 2000.

[57] Hodgkin, A. L., and Huxley, A. F. (1952) A quantitative description of membrane current and its application to conduction and excitation in nerve. *J. Physiol. 117*, 500–544.

[58] del Castillo, J., and Katz, B. (1957) Interaction at end-plate receptors between different choline derivatives. *Proc. R. Soc. Lond. B Biol. Sci. 146*, 369–381.

[59] Jancsó, N., Jancsó-Gábor, A., and Szolcsányi, J. (1967) Direct evidence for neurogenic inflammation and its prevention by denervation and by pretreatment with capsaicin. *Br. J. Pharmacol. Chemother. 31*, 138–151.

[60] Wood, J. N., Winter, J., James, I. F., Rang, H. P., Yeats, J., and Bevan, S. (1988) Capsaicin-induced ion fluxes in dorsal root ganglion cells in culture. *J. Neurosci. 8*, 3208–3220.

[61] Bevan, S., and Szolcsányi, J. (1990) Sensory neuron-specific actions of capsaicin: mechanisms and applications. *Trends Pharmacol. Sci. 11*, 330–333.

[62] LaMotte, R. H., Lundberg, L. E. R., and Torebjörk, H. E. (1992) Pain, hyperalgesia and activity in nociceptive C units in humans after intradermal injection of capsaicin. *J. Physiol. 448*, 749–764.

[63] Torebjörk, H. E., Lundberg, L. E., and LaMotte, R. H. (1992) Central changes in processing of mechanoreceptive input in capsaicin-induced secondary hyperalgesia in humans. *J. Physiol. 448*, 765–780.

[64] Caterina, M. J., Schumacher, M. A., Tominaga, M., Rosen, T. A., Levine, J. D., and Julius, D. (1997) The capsaicin receptor: a heat-activated ion channel in the pain pathway. *Nature 389*, 816–824.

[65] Tominaga, M., Caterina, M. J., Malmberg, A. B., Rosen, T. A., Gilbert, H., Skinner, K., Raumann, B. E., Basbaum, A. I., and Julius, D. (1998) The cloned capsaicin receptor integrates multiple pain-producing stimuli. *Neuron 21*, 531–543.

[66] Tominaga, M., and Caterina, M. J. (2004) Thermosensation and pain. *J. Neurobiol. 61*, 3–12.

[67] Conway, S. J. (2008) TRPing the switch on pain: an introduction to the chemistry and biology of capsaicin and TRPV1. *Chem. Soc. Rev. 37*, 1530–1545.

[68] Palazzo, E., Luongo, L., de Novellis, V., Rossi, F., Marabese, I., and Maione, S. (2012) Transient receptor potential vanilloid type 1 and pain development. *Curr. Opin. Pharmacol. 12*, 9–17.

[69] Szallasi, A., and Blumberg, P. M. (1999) Vanilloid (Capsaicin) receptors and mechanisms. *Pharmacol. Rev. 51*, 159–212.

[70] Clapham, D. E. (2003) TRP channels as cellular sensors. *Nature 426*, 517–524.

[71] Patapoutian, A., Tate, S., and Woolf, C. J. (2009) Transient receptor potential channels: targeting pain at the source. *Nat. Rev. Drug Discov. 8*, 55–68.

[72] Welch, J. M., Simon, S. A., and Reinhart, P. H. (2000) The activation mechanism of rat vanilloid receptor 1 by capsaicin involves the pore domain and differs from the activation by either acid or heat. *Proc. Natl. Acad. Sci. U. S. A. 97*, 13889–13894.

[73] Hellwig, N., Plant, T. D., Janson, W., Schäfer, M., Schultz, G., and Schaefer, M. (2004) TRPV1 acts as proton channel to induce acidification in nociceptive neurons. *J. Biol. Chem. 279*, 34553–34561.

[74] Voets, T., Droogmans, G., Wissenbach, U., Janssens, A., Flockerzi, V., and Nilius, B. (2004) The principle of temperature-dependent gating in cold- and heat-sensitive TRP channels. *Nature 430*, 748–754.

[75] Clapham, D. E., Julius, D., Montell, C., and Schultz, G. (2005) International Union of Pharmacology. XLIX. Nomenclature and structure-function relationships of transient receptor potential channels. *Pharmacol. Rev. 57*, 427–450.

[76] Dhaka, A., Viswanath, V., and Patapoutian, A. (2006) TRP ion channels and temperature sensation. *Annu. Rev. Neurosci. 29*, 135–161.

[77] Ryu, S., Liu, B., Yao, J., Fu, Q., and Qin, F. (2007) Uncoupling proton activation of vanilloid receptor TRPV1. *J. Neurosci. 27*, 12797–12807.

[78] Matta, J. A., and Ahern, G. P. (2007) Voltage is a partial activator of rat thermosensitive TRP channels. *J. Physiol. 585*, 469–482.

[79] Bohlen, C. J., Priel, A., Zhou, S., King, D., Siemens, J., and Julius, D. (2010) A bivalent tarantula toxin activates the capsaicin receptor, TRPV1, by targeting the outer pore domain. *Cell 141*, 834–845.

[80] Baez-Nieto, D., Castillo, J. P., Dragicevic, C., Alvarez, O., and Latorre, R. In *Transient receptor potential channels*; Islam, M. S., Ed.; Adv. Exp. Med. Biol.; Springer: New York, 2011; Vol. 704; Chapter 26: Thermo-TRP channels: biophysics of polymodal receptors., pp 469–490.

[81] Jordt, S.-E., and Julius, D. (2002) Molecular basis for species-specific sensitivity to "hot" chili peppers. *Cell 108*, 421–430.

[82] Tewksbury, J. J., Nabhan, G. P., Norman, D., Suzán, H., Tuxill, J., and Donovan, J. (1999) In situ conservation of wild chiles and their biotic associates. *Conserv. Biol. 13*, 98–107.

[83] Tewksbury, J. J., and Nabhan, G. P. (2001) Seed dispersal. Directed deterrence by capsaicin in chilies. *Nature 412*, 403–404.

[84] Jung, J., Hwang, S. W., Kwak, J., Lee, S. Y., Kang, C. J., Kim, W. B., Kim, D., and Oh, U. (1999) Capsaicin binds to the intracellular domain of the capsaicin-activated ion channel. *J. Neurosci. 19*, 529–538.

[85] Brauchi, S., Orta, G., Salazar, M., Rosenmann, E., and Latorre, R. (2006) A hot-sensing cold receptor: C-terminal domain determines thermosensation in transient receptor potential channels. *J. Neurosci. 26*, 4835–4840.

[86] Yang, F., Cui, Y., Wang, K., and Zheng, J. (2010) Thermosensitive TRP channel pore turret is part of the temperature activation pathway. *Proc. Natl. Acad. Sci. U. S. A. 107*, 7083–7088.

[87] Moiseenkova-Bell, V. Y., Stanciu, L. A., Serysheva, I. I., Tobe, B. J., and Wensel, T. G. (2008) Structure of TRPV1 channel revealed by electron cryomicroscopy. *Proc. Natl. Acad. Sci. U. S. A. 105*, 7451–7455.

[88] Lishko, P. V., Procko, E., Jin, X., Phelps, C. B., and Gaudet, R. (2007) The ankyrin repeats of TRPV1 bind multiple ligands and modulate channel sensitivity. *Neuron 54*, 905–918.

[89] Koplas, P. A., Rosenberg, R. L., and Oxford, G. S. (1997) The role of calcium in the desensitization of capsaicin responses in rat dorsal root ganglion neurons. *J. Neurosci. 17*, 3525–3537.

[90] Liu, L., and Simon, S. A. (2000) Capsaicin, acid and heat-evoked currents in rat trigeminal ganglion neurons: relationship to functional VR1 receptors. *Physiol. Behav. 69*, 363–378.

[91] Numazaki, M., Tominaga, T., Takeuchi, K., Murayama, N., Toyooka, H., and Tominaga, M. (2003) Structural determinant of TRPV1 desensitization interacts with calmodulin. *Proc. Natl. Acad. Sci. U. S. A. 100*, 8002–8006.

[92] Rosenbaum, T., Gordon-Shaag, A., Munari, M., and Gordon, S. E. (2004) Ca^{2+}/calmodulin modulates TRPV1 activation by capsaicin. *J. Gen. Physiol. 123*, 53–62.

[93] Liu, B., Zhang, C., and Qin, F. (2005) Functional recovery from desensitization of vanilloid receptor TRPV1 requires resynthesis of phosphatidylinositol 4,5-bisphosphate. *J. Neurosci. 25*, 4835–4843.

[94] Niemeyer, B. A. (2005) Structure-function analysis of TRPV channels. *Naunyn-Schmiedeberg's Arch. Pharmacol. 371*, 285–294.

[95] Huang, J., Zhang, X., and McNaughton, P. A. (2006) Modulation of temperature-sensitive TRP channels. *Semin. Cell Dev. Biol. 17*, 638–645.

[96] Novakova-Tousova, K., Vyklicky, L., Susankova, K., Benedikt, J., Samad, A., Teisinger, J., and Vlachova, V. (2007) Functional changes in the vanilloid receptor subtype 1 channel during and after acute desensitization. *Neuroscience 149*, 144–154.

[97] Studer, M., and McNaughton, P. A. (2010) Modulation of single-channel properties of TRPV1 by phosphorylation. *J. Physiol. 588*, 3743–3756.

[98] Tominaga, M., Wada, M., and Masu, M. (2001) Potentiation of capsaicin receptor activity by metabotropic ATP receptors as a possible mechanism for ATP-evoked pain and hyperalgesia. *Proc. Natl. Acad. Sci. U. S. A. 98*, 6951–6956.

[99] Ryu, S., Liu, B., and Qin, F. (2003) Low pH potentiates both capsaicin binding and channel gating of VR1 receptors. *J. Gen. Physiol. 122*, 45–61.

[100] Neelands, T. R., Jarvis, M. F., Han, P., Faltynek, C. R., and Surowy, C. S. (2005) Acidification of rat TRPV1 alters the kinetics of capsaicin responses. *Mol. Pain 1*, 28.

[101] Veldhuis, N. A., Lew, M. J., Abogadie, F. C., Poole, D. P., Jennings, E. A., Ivanusic, J. J., Eilers, H., Bunnett, N. W., and McIntyre, P. (2012) N-glycosylation determines ionic permeability and desensitization of the TRPV1 capsaicin receptor. *J. Biol. Chem. 287*, 21765–21772.

[102] Virginio, C., MacKenzie, A., Rassendren, F. A., North, R. A., and Surprenant, A. (1999) Pore dilation of neuronal P2X receptor channels. *Nat. Neurosci. 2*, 315–321.

[103] Khakh, B. S., Bao, X. R., Labarca, C., and Lester, H. A. (1999) Neuronal P2X transmitter-gated cation channels change their ion selectivity in seconds. *Nat. Neurosci. 2*, 322–330.

[104] Chung, M.-K., Güler, A. D., and Caterina, M. J. (2008) TRPV1 shows dynamic ionic selectivity during agonist stimulation. *Nat. Neurosci. 11*, 555–564.

[105] Chen, J., Kim, D., Bianchi, B. R., Cavanaugh, E. J., Faltynek, C. R., Kym, P. R., and Reilly, R. M. (2009) Pore dilation occurs in TRPA1 but not in TRPM8 channels. *Mol. Pain 5*, 3.

[106] Banke, T. G., Chaplan, S. R., and Wickenden, A. D. (2010) Dynamic changes in the TRPA1 selectivity filter lead to progressive but reversible pore dilation. *Am. J. Physiol. Cell Physiol. 298*, C1457–C1468.

[107] Gunthorpe, M. J., Benham, C. D., Randall, A., and Davis, J. B. (2002) The diversity in the vanilloid (TRPV) receptor family of ion channels. *Trends. Pharmacol. Sci. 23*, 183–191.

[108] Szallasi, A., and Appendino, G. (2004) Vanilloid receptor TRPV1 antagonists as the next generation of painkillers. Are we putting the cart before the horse? *J. Med. Chem. 47*, 2717–2723.

[109] Immke, D. C., and Gavva, N. R. (2006) The TRPV1 receptor and nociception. *Semin. Cell Dev. Biol. 17*, 582–591.

[110] Holzer, P. (2008) The pharmacological challenge to tame the transient receptor potential vanilloid-1 (TRPV1) nocisensor. *Br. J. Pharmacol. 155*, 1145–1162.

[111] Bley, K. R. In *Vanilloid receptor TRPV1 in drug discovery: targeting pain and other pathological disorders*; Gomtsyan, A., and Faltynek, C. R., Eds.; John Wiley & Sons: Hoboken, New Jersey, 2010; Chapter 13: TRPV1 agonist approaches for pain management, pp 325–347.

[112] Hodgkin, A. L., and Huxley, A. F. (1952) Currents carried by sodium and potassium ions through the membrane of the giant axon of *Loligo*. *J. Physiol. 116*, 449–472.

[113] Hodgkin, A. L., and Huxley, A. F. (1952) The components of membrane conductance in the giant axon of *Loligo*. *J. Physiol. 116*, 473–496.

[114] Hodgkin, A. L., and Huxley, A. F. (1952) The dual effect of membrane potential on sodium conductance in the giant axon of *Loligo*. *J. Physiol. 116*, 497–506.

[115] Hodgkin, A. L., Huxley, A. F., and Katz, B. (1952) Measurement of current-voltage relations in the membrane of the giant axon of *Loligo*. *J. Physiol. 116*, 424–448.

[116] Penner, R. In *Single-channel recording*, 2nd ed.; Sakmann, B., and Neher, E., Eds.; Plenum Press: New York, 1995; Chapter 1: A practical guide to patch clamping, pp 3–30.

[117] Marty, A., and Neher, E. In *Single-channel recording*, 2nd ed.; Sakmann, B., and Neher, E., Eds.; Plenum Press: New York, 1995; Chapter 2: Tight-seal whole-cell recording, pp 31–52.

[118] Molleman, A. *Patch clamping: an introductory guide to patch clamp electrophysiology*; John Wiley & Sons: Chichester, 2003.

[119] Sigworth, F. J. In *Single-channel recording*, 2nd ed.; Sakmann, B., and Neher, E., Eds.; Plenum Press: New York, 1995; Chapter 4: Electronic design of the patch clamp, pp 95–127.

[120] Nyquist, H. (1928) Thermal agitation of electric charge in conductors. *Phys. Rev. 32*, 110–113.

[121] Heinemann, S. H. In *Single-channel recording*, 2nd ed.; Sakmann, B., and Neher, E., Eds.; Plenum Press: New York, 1995; Chapter 3: Guide to data aquisition and analysis, pp 53–91.

[122] Brody, J. P., Yager, P., Goldstein, R. E., and Austin, R. H. (1996) Biotechnology at low Reynolds numbers. *Biophys. J. 71*, 3430–3441.

[123] Squires, T. M., and Quake, S. R. (2005) Microfluidics: Fluid physics at the nanoliter scale. *Rev. Mod. Phys. 77*, 977–1026.

[124] Weibel, D. B., and Whitesides, G. M. (2006) Applications of microfluidics in chemical biology. *Curr. Opin. Chem. Biol. 10*, 584–591.

[125] Whitesides, G. M. (2006) The origins and the future of microfluidics. *Nature 442*, 368–373.

[126] Purcell, E. M. (1977) Life at low Reynolds number. *Am. J. Phys. 45*, 3–11.

[127] Colquhoun, D., Jonas, P., and Sakmann, B. (1992) Action of brief pulses of glutamate on AMPA/kainate receptors in patches from different neurones of rat hippocampal slices. *J. Physiol. 458*, 261–287.

[128] Sinclair, J., Pihl, J., Olofsson, J., Karlsson, M., Jardemark, K., Chiu, D. T., and Orwar, O. (2002) A cell-based bar code reader for high-throughput screening of ion channel-ligand interactions. *Anal. Chem. 74*, 6133–6138.

[129] Sinclair, J., Olofsson, J., Phil, J., and Orwar, O. (2003) Stabilization of high-resistance seals in patch-clamp recordings by laminar flow. *Anal. Chem. 75*, 6718–6722.

[130] Olofsson, J., Pihl, J., Sinclair, J., Sahlin, E., Karlsson, M., and Orwar, O. (2004) A microfluidics approach to the problem of creating separate solution environments accessible from macroscopic volumes. *Anal. Chem. 76*, 4968–4976.

[131] Sinclair, J., Granfeldt, D., Pihl, J., Millingen, M., Lincoln, P., Farre, C., Peterson, L., and Orwar, O. (2006) A biohybrid dynamic random access memory. *J. Am. Chem. Soc. 128*, 5109–5113.

[132] Pihl, J., Sinclair, J., Sahlin, E., Karlsson, M., Petterson, F., Olofsson, J., and Orwar, O. (2005) Microfluidic gradient-generating device for pharmacological profiling. *Anal. Chem. 77*, 3897–3903.

[133] Pihl, J., Karlsson, M., and Chiu, D. T. (2005) Microfluidic technologies in drug discovery. *Drug Discov. Today 10*, 1377–1383.

[134] Olofsson, J., Bridle, H., Sinclair, J., Granfeldt, D., Sahlin, E., and Orwar, O. (2005) A chemical waveform synthesizer. *Proc. Natl. Acad. Sci. U. S. A. 102*, 8097–8102.

[135] Granfeldt, D., Sinclair, J., Millingen, M., Farre, C., Lincoln, P., and Orwar, O. (2006) Controlling desensitized states in ligand-receptor interaction studies with cyclic scanning patch-clamp protocols. *Anal. Chem. 78*, 7947–7953.

[136] Bridle, H., Olofsson, J., Jesorka, A., and Orwar, O. (2007) Automated control of local solution environments in open-volume microfluidics. *Anal. Chem. 79*, 9286–9293.

[137] Bridle, H., Millingen, M., and Jesorka, A. (2008) On-chip fabrication to add temperature control to a microfluidic solution exchange system. *Lab. Chip 8*, 480–483.

[138] Chooneea, D., Karlsson, R., Encheva, V., Arnold, C., Appleton, H., and Shah, H. (2010) Elucidation of the outer membrane proteome of Salmonella enterica serovar Typhimurium utilising a lipid-based protein immobilization technique. *BMC Microbiol. 10*, 44.

[139] Hansson, S. F., Henriksson, Å., Johansson, L., Korsgren, O., Eriksson, J. W., Tornqvist, H., and Davidsson, P. (2010) Membrane protein profiling of human islets of Langerhans using several extraction methods. *Clin. Proteomics 6*, 195–207.

[140] Padliya, N. D., Bhatia, M. B., Hofgärtner, W. T., and Hariri, R. J. (2010) Improving the depth of coverage in membrane proteomic studies through the use of lipid-based protein immobilization technology in parallel with methanol-facilitated solubilisation. *Anal. Methods 2*, 539–545.

[141] Karlsson, R., Davidson, M., Svensson-Stadler, L., Karlsson, A., Olesen, K., Carlsohn, E., and Moore, E. R. B. (2012) Strain-level typing and identification of bacteria using mass spectrometry-based proteomics. *J. Proteome Res.*

[142] O'Neill, M. E. (1968) A sphere in contact with a plane wall in a slow linear shear flow. *Chem. Eng. Sci. 23*, 1293 – 1298.

[143] Weibel, D. B., Diluzio, W. R., and Whitesides, G. M. (2007) Microfabrication meets microbiology. *Nat. Rev. Microbiol. 5*, 209–218.

[144] Lakowicz, J. R. *Principles of fluorescence spectroscopy*, 3rd ed.; Springer: New York, 2006.

[145] Bixon, M., and Jortner, J. (1968) Intramolecular radiationless transitions. *J. Chem. Phys. 48*, 715–726.

[146] Jabłoński, A. (1933) Efficiency of anti-Stokes fluorescence in dyes. *Nature 131*, 839–840.

[147] Johnson, I. D. In *Handbook of biological confocal microscopy*, 3rd ed.; Pawley, J. B., Ed.; Springer: New York, 2006; Chapter 17: Practical considerations in the selection and application of fluorescent probes, pp 353–367.

[148] Grynkiewicz, G., Poenie, M., and Tsien, R. Y. (1985) A new generation of Ca^{2+} indicators with greatly improved fluorescence properties. *J. Biol. Chem. 260*, 3440–3450.

[149] Idziorek, T., Estaquier, J., De Bels, F., and Ameisen, J. C. (1995) YOPRO-1 permits cytofluorometric analysis of programmed cell death (apoptosis) without interfering with cell viability. *J. Immunol. Methods 185*, 249–258.

[150] Minsky, M. Microscopy apparatus. U.S. Patent 3013467, 1961.

[151] Paddock, S. W. In *Principles and techniques of biochemistry and molecular biology*, 6th ed.; Wilson, K., and Walker, J., Eds.; Cambridge University Press: New York, 2005; Chapter 4: Microscopy, pp 131–165.

[152] Inoué, S. In *Handbook of biological confocal microscopy*, 3rd ed.; Pawley, J. B., Ed.; Springer: New York, 2006; Chapter 1: Foundations of confocal scanned imaging in light microscopy, pp 1–19.

[153] Wasinger, V. C., Cordwell, S. J., Cerpa-Poljak, A., Yan, J. X., Gooley, A. A., Wilkins, M. R., Duncan, M. W., Harris, R., Williams, K. L., and Humphery-Smith, I. (1995) Progress with gene-product mapping of the Mollicutes: Mycoplasma genitalium. *Electrophoresis 16*, 1090–1094.

[154] Anderson, N. L., and Anderson, N. G. (1998) Proteome and proteomics: new technologies, new concepts, and new words. *Electrophoresis 19*, 1853–1861.

[155] Blackstock, W. P., and Weir, M. P. (1999) Proteomics: quantitative and physical mapping of cellular proteins. *Trends Biotechnol. 17*, 121–127.

[156] Watson, J. T., and Sparkman, O. D. *Introduction to mass spectrometry: instrumentation, applications, and strategies for data interpretation*, 4th ed.; John Wiley & Sons: Chichester, 2007.

[157] Aebersold, R., and Goodlett, D. R. (2001) Mass spectrometry in proteomics. *Chem. Rev. 101*, 269–295.

[158] Aebersold, R., and Mann, M. (2003) Mass spectrometry-based proteomics. *Nature 422*, 198–207.

[159] Washburn, M. P., Wolters, D., and Yates, J. R. (2001) Large-scale analysis of the yeast proteome by multidimensional protein identification technology. *Nat. Biotechnol. 19*, 242–247.

[160] Steen, H., and Mann, M. (2004) The ABC's (and XYZ's) of peptide sequencing. *Nat. Rev. Mol. Cell Biol. 5*, 699–711.

[161] Stengel, F., Aebersold, R., and Robinson, C. V. (2012) Joining forces: integrating proteomics and cross-linking with the mass spectrometry of intact complexes. *Mol. Cell Proteomics 11*, R111.014027.

[162] Edman, P. (1950) Method for determination of the amino acid sequence in peptides. *Acta Chem. Scand. 4*, 283–293.

[163] de Hoffmann, E., and Stroobant, V. *Mass spectrometry: principles and applications*, 3rd ed.; John Wiley & Sons: Chichester, 2007.

[164] Makarov, A., and Scigelova, M. (2010) Coupling liquid chromatography to Orbitrap mass spectrometry. *J. Chromatogr. A 1217*, 3938–3945.

[165] Moore, R. E., Young, M. K., and Lee, T. D. (2002) Qscore: an algorithm for evaluating SEQUEST database search results. *J. Am. Soc. Mass Spectrom. 13*, 378–386.

[166] Elias, J. E., and Gygi, S. P. (2007) Target-decoy search strategy for increased confidence in large-scale protein identifications by mass spectrometry. *Nat. Methods 4*, 207–214.

[167] Navarro, P., and Vázquez, J. (2009) A refined method to calculate false discovery rates for peptide identification using decoy databases. *J. Proteome Res. 8*, 1792–1796.

[168] Hubbard, S. J. (1998) The structural aspects of limited proteolysis of native proteins. *Biochim. Biophys. Acta 1382*, 191–206.

[169] Sides, C. R., Liyanage, R., Lay, J. O., Jr, Philominathan, S. T. L., Matsushita, O., and Sakon, J. (2012) Probing the 3-D structure, dynamics, and stability of bacterial collagenase collagen binding domain (apo- versus holo-) by limited proteolysis MALDI-TOF MS. *J. Am. Soc. Mass Spectrom. 23*, 505–519.

[170] Scott, R. E. (1976) Plasma membrane vesiculation: a new technique for isolation of plasma membranes. *Science 194*, 743–745.

[171] Scott, R. E., Perkins, R. G., Zschunke, M. A., Hoerl, B. J., and Maercklein, P. B. (1979) Plasma membrane vesiculation in 3T3 and SV3T3 cells. I. Morphological and biochemical characterization. *J. Cell Sci. 35*, 229–243.

[172] Scott, R. E., and Maercklein, P. B. (1979) Plasma membrane vesiculation in 3T3 and SV3T3 cells. II. Factors affecting the process of vesiculation. *J. Cell Sci. 35*, 245–252.

[173] Bauer, B., Davidson, M., and Orwar, O. (2009) Proteomic analysis of plasma membrane vesicles. *Angew. Chem. Int. Edit. 48*, 1656–1659.

[174] Rigaud, J. L., Pitard, B., and Levy, D. (1995) Reconstitution of membrane proteins into liposomes: application to energy-transducing membrane proteins. *Biochim. Biophys. Acta 1231*, 223–246.

[175] Dounce, A. L. *The nucleic acids: chemistry and biology*; Academic Press: New York, 1955; Vol. 2; Chapter 18: The isolation and composition of cell nuclei and nucleoli, pp 93–154.